International Journal of Modern Physics B
Vol. 32, No. 17 (2018) 1840036 (38 pages)

DOI: 10.1142/S0217979218400362

Experimental and theoretical aspects of thermodynamic properties of quasi-1D and quasi-2D organic conductors and superconductors

Y. Nakazawa*

Department of Chemistry, Osaka University,
Toyonaka, Osaka 560-0043, Japan
nakazawa@chem.sci.osaka-u.ac.jp

S. Kruchinin

Bogolyubov Institute for Theoretical Physics,
National Academy of Sciences of Ukraine,
03143 Kiev, Ukraine
skruchin@i.com.ua

Accepted 7 February 2018
Published 12 April 2018

We deal with thermodynamic features of organic conductors and superconductors where itinerant π-electrons/holes released from organic molecules are playing essential roles for electronic properties. Since they are low-dimensional electronic systems with relatively soft lattice framework, they show variety of phenomena related to electron correlations and electron–lattice coupling. The drastic changes of conductive and magnetic properties owing to quantum features of π-electrons can be induced by external perturbations such as magnetic/electric field, pressure, etc. It is especially emphasized that the possible mechanism and relation with other phenomena of the superconductivity in π-electrons system remains to be one of the interesting research areas in fundamental condensed matter science. In this review paper, we consider several topics of organic conductors and superconductors from the standpoints of thermodynamic experiments, data analyses and theories performed up to now. Starting from the overall picture of the electronic states in charge transfer complexes, thermodynamic properties of the quasi-one-dimensional systems, quasi-two-dimensional systems and π–d interacting systems are reviewed. The thermodynamic parameters of the superconductive compounds in them are compared and discussed. The relations with crystal structures, electronic states, phase diagram and other experiments are also discussed in comparison with these thermodynamic properties. The possible pairing symmetries in organic superconductors and some models are mentioned in the last part. This review deals with a wide scope of theoretical and experimental topics in superconductivity in molecule-based conductive systems.

Keywords: Organic superconductors; thermodynamics; specific heat; mechanism of pairing; symmetry of pairing.

PACS numbers: 65.40.Ba, 74.25.Bt, 74.70.kn

*Corresponding author.

1. Introduction

The research on the physical features of molecule-based conducting systems has been extensively performed in these decades from the standpoints of electron correlation and electron–lattice interactions in low-dimensional system. Since these compounds are chemically synthesized metals and semiconductors which do not exist in nature, they are recognized as promising materials to give novel features related to electron correlation and electron–lattice coupled systems and to give possible application as molecular devices. In general, organic molecules have self-contained closed-shell structures, where two electrons with alternative spins occupy their highest occupied molecular orbitals (HOMOs). Therefore, charge carriers should be produced by introducing electrons into the lowest unoccupied molecular orbitals (LUMOs) or removing electrons from HOMOs. There are at least three strategies to make conducting networks in organic solids performed up to now and also superconductivity of π-electrons is realized. The first one is to introduce mobile carriers by doping a cation or an anion in a neutral crystal of π-conjugated molecules. An early work on halogen doping in solid perylene is known as the first observation of an organic semiconducting system.[1] The doping in neutral crystals of C_{60}, etc. by alkali ions such as pottassium (K), Rb and Cs is known to produce superconductivity at 20–30 K.[2,3] The intercalation by metal dopants in graphite produces superconductivity in C_8K ($T_c \approx 0.14$ K), C_2Na ($T_c \approx 5$ K), C_6Yb ($T_c \approx 6.5$ K) and C_6Ca ($T_c \approx 11.5$ K).[4,5] Recently, K doping in solid-state picene is attracting interests as a novel organic superconductor.[6] The well-known strategy to get conducting systems is to make charge transfer complexes of donors and acceptors. There are many organic conductors and superconductors which have been studied by thermodynamic techniques as we survey in this paper.[7–9] Since the molecular structures and stacking directions have large anisotropy, the electronic bands produced by the overlap of the molecular orbitals of neighboring molecules have low-dimensional characters in them. The third strategy is to introduce a carrier in the interface of organic crystals and insulating layers by making field-effect transistor structures.[10,11] Using naphthalene, pentacene, rubrene and other organic molecules, the carrier's mobility and functionality as devices in the semiconductive region in the interface area are studied extensively.

Heat capacity is an important physical property to explore fundamental researches of organic conductors and superconductors.[12,13] One can detect various types of phase transitions by measuring heat capacity as a function of temperature. The determination of transition entropy and enthalpy can give direct information on degrees of ordering of microscopic freedoms existing in molecules, atoms and conduction electrons interacting each other. Heat capacity measurements performed with various external parameters controls can give further information of magnetic/electric fields and pressures-induced new phases. Magnetic-field-induced phenomena such as field-induced superconductivity and unusual behavior of superconductivities and pressure-induced neutral–ionic phase transitions are the targets

of thermodynamic studies. In addition to these points, effective usage of thermodynamic measurements at low-temperature region is useful to clarify the nature of ground states and low-energy excitations (LEEs) from them. The high-precision heat capacity at low temperature can give electronic information, for example, like γ-term, Debye temperature and unusual phase transition due to quantum phenomenon occurring in low-energy region. The quasi-particle excitations in superconducting ground state can give information on gap structure and pairing mechanism.

A serious point for measuring heat capacity of organic conductors is difficulty to get large amount of samples. Crystals of organic charge transfer systems are yielded by electrochemical oxidation/reduction or diffusion method from solutions of organic molecules with their counter ions in organic solvent. The typical size of single crystal is about 1–100 μg. To get large amount of sample or to get large single crystals suitable for heat capacity measurements is a difficult task, despite that high-quality single crystals with relatively long mean-free paths suitable for determining microstructure of Fermi surfaces can be obtained from them. Therefore the heat capacity measurements are mainly performed by thermal relaxation method or AC modulation method depending on the size of the crystals. The adiabatic or semi-adiabatic methods are also performed for sets of many pieces of single crystals or powdered samples ($\sim$100 mg) sealed within a sample holder with ^{4}He exchange gas. The data of adiabatic calorimetry for organic conductors are limited to several cases.

In this review paper, we mainly discuss the thermodynamic properties of molecule-based conducting and superconducting charge transfer compounds from the standpoints of experimental and theoretical works. First, we explain the electronic structures of organic donors/acceptors-based superconductive compounds. Then, we summarize the experimental thermodynamic works performed up to now for several systems which are attracting interests in relation to unconventional superconductive features. Theoretical model calculation to explain the superconductive features is presented in the last part.

1.1. *Electronic structures of charge transfer complexes of donor/acceptors with their counter ions*

In this subsection, we explain the electronic structures of molecular charge transfer complexes in terms of electron correlations. The charge transfer complexes consisting of donor or acceptor molecules with their counter ions are recognized as good candidates to give conducting properties with quasi-one-dimensional (quasi-1D) or quasi-two-dimensional (quasi-2D) structures with electron correlations, since they have layered structure of organic molecules and counter ions as shown in Fig. 1. Numerous complexes which have simple composition of 2:1 (D_2X or A_2Y) or 1:1 (DX or AY), where D and A denote donor and acceptor molecules and X and Y represent counter anions and cations, are synthesized and their physical properties have been studied. The complexes with more complicated chemical compositions and those containing organic solvents such as THF, CH_2Cl_2, H_2O, etc. in

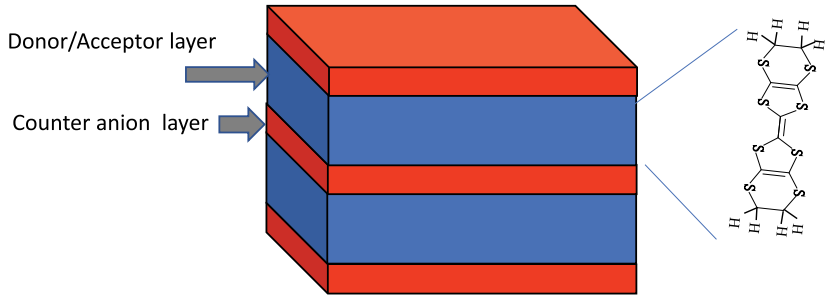

Fig. 1. (Color online) A schematic view of the organic charge transfer complexes consisting of organic donor/acceptor layers and their counter ion layers. Organic molecules and counter ions have segregate stacking to form 2D layered structure. The molecular arrangement of the organic layers has rich varieties. In the case of TMTTF/TMTSF face to face stacking of donor molecules forms quasi-1D electronic structure, while the 2D electronic structures are stabilized in the case of BEDT-TTF and BETS complexes.

the crystals are also known up to now. However, considering the electrochemical oxidation/reduction processes in the crystal growth in solutions, the 2:1 composition seems to be appropriate in the donor/acceptor and counter ions combination. The 2:1 complexes are also well known and widely studied, because they give many conducting, semiconducting and sometimes magnetic systems. Various types of electronic ground states such as SDW, CDW, antiferromagnetic (AF), charge-ordered (CO) and superconductive ones are known to exist around metallic phase. They are related each other to produce variety of quantum mechanical ground states. These complexes in general have segregated stacking structures and conductivity appears in donor/acceptor sheet or column. The electronic states are related to the arrangement in the organic molecules.[14–16] In the following sections, we focus on the thermodynamic properties of typical 2:1 complexes consisting of several organic donor molecules such as BEDT-TTF, BETS and tetramethyltetraselenafulvalene/tetramethyltetrathiafulvalene (TMTSF/TMTTF), with their counter ions.

The 2:1 complexes of BEDT-TTF and BETS are appropriate research stages for studying the two-dimensional (2D) electronic systems, while the TMTTF/TMTSF complexes are considered as quasi-1D systems. Although the smaller TMTTF/TMTSF donor molecules stack with face to face direction despite forming a layered-type structure, their physical properties are explained by the quasi-1D phase diagram.[17] In the case of BEDT-TTF and BETS molecules, the S–S and Se–Se contacts between neighboring molecules cause a rather large transverse overlap of molecular orbitals, as well as the transfer energy in stacking direction to face directly. This leads to the 2D network arrangement in the donor layers. In fact in the metallic compounds with $(\text{BEDT-TTF})_2X$ and BETS_2X, the structure of cylindrical Fermi surface has been studied by Shubnikov–de Haas (SdH) and de Haas–van Alphen (dHvA) oscillations. Recently, detection of quantum oscillation in electron density of states by changing the magnetic fields has been successfully probed by C_pT^{-1} in heat capacity measurements at extremely low-temperature

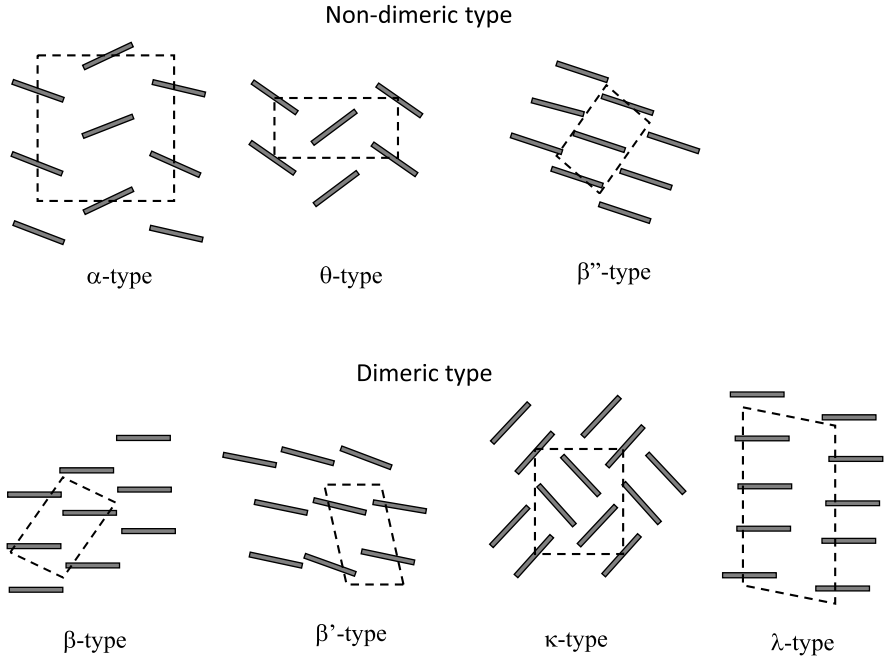

Fig. 2. Schematic views of molecular arrangements of organic charge transfer complexes. The difference of the structures is denoted using the Greek characters. The types of the structures are categorized as nondimeric type and dimeric type.

region. Thermodynamic discussion in relevance to the structure in Fermi surface becomes possible.[18,19]

In discussing the variety of electronic properties in these organic charge transfer complexes, understanding the systematic relation between donor packing structure and physical properties is important. The variation of donor arrangement in the 2D plane is assorted by using Greek characters. Typical structures of BEDT-TTF molecules in 2D plane are shown in Fig. 2. It is well-known that degree of dimerization is a good criterion to classify the electronic structures of 2:1 compounds. When intradimer coupling (t_{dimer}) is larger than other interdimer interactions as in the case of κ-, β-, β'- or λ-type arrangements, a dimerization gap appears in the center of HOMO band. The originally quarter-filled band in 2:1 complex is therefore considered as effectively half-filled one of the upper HOMO band. The peculiar feature of these systems is an appearance of Mott–Hubbard physics related to the competition of onsite electron correlation U and magnitude of the width of the upper HOMO band. The superconductivity realized in these dimer-based systems is known to give relatively high transition temperature exceeding 10 K. It is discussed in terms of unconventional superconductors in which the spin degrees of freedom is playing an important role. In the case of nondimerized complexes, namely for example α-, θ- and β''-type structures in Fig. 10, the band-filling is 3/4 and metallic nature is stabilized at low temperatures. The good metallic state with

long mean-free path gives an appropriate stage to consider Fermi surface structure and nesting problems in the one-dimensional (1D) and 2D Fermi surfaces. In these nondimeric systems, the electron correlation appears as the intersite Coulomb interaction term V and this interaction causes disproportionation in charge distribution sometimes recognized as a Wigner-type crystallization of electrons or holes. The CO ground state or valence-bond solid (VBS) ground state is investigated as manifestation of such kind of electron correlations. The superconductive phase that appears in θ- or β''-structure is discussed in terms of charge fluctuation-induced one. The unconventional nature of the superconductivity is still an open question in organics and thermodynamic works are considered as important to study the gap anisotropy through the low-energy excitations. The relation between molecular packing and electronic properties is explained theoretically in several works.[14,15]

2. Thermodynamic Properties of $(TMTSF)_2X$ and $(TMTTF)_2X$ Systems

The compounds belonging to $(TMTCF)_2X$ family, where TMTCF represents TMTTF or TMTSF, are known to have quasi-1D character like TTF-TCNQ. These donor molecules were developed as derivatives of TTF to stabilize molecular stacking in conducting chain and intercolumn interactions. They crystallize into layered structure of donors and counter anions with a composition of 2:1 similar to the case of BEDT-TTF and BETS systems. The crystal structure of these complexes is triclinic with $P\bar{1}$-symmetry for the $(TMTSF)_2PF_6$ case.[20] In this system, donor molecules form a column structure in the layers to provide strongly anisotropic in-plane transport properties. The ratio of transfer energies in the three directions in the crystal shown in Fig. 10 is t_a:t_b:t_c = 300:10:1, where that in the stacking direction of a-axis is about $t_a = 0.38$ eV. In this direction, donor molecules are weakly dimerized and therefore onsite Coulomb interaction term U in the dimer unit and intersite Coulomb interaction term V between neighboring molecules (both intradimer and interdimer) are important in understanding the electronic structures. There are many varieties in the type of counter anions, which are classified into spherical (PF_6^-, AsF_6^-, SbF_6^-, TaF_6^-), tetrahedral (BF_4^-, ClO_4^-, ReO_4^-) and triangular (NO_3^-) ones. The polymeric anions of SCN^- and atoms of Br^- are known and studied extensively.

In 1980, the first observation of superconductivity among organic systems was reported in $(TMTSF)_2PF_6$ at 0.9 K under an applied pressure of 1.2 GPa.[21] $(TMTSF)_2ClO_4$ was reported as an ambient-pressure superconductor with T_c = 1.4 K in 1982.[22] Including this superconductive phase appearing in the metal region, the series of TMTSF and TMTTF compounds were found to show sequential changes of electronic ground states with controlling external pressures or chemical pressures by anion size. The phase diagram is established by Jérome *et al.*[17,23] The SDW compounds and co-workers $(TMTSF)_2X$ with various X show superconductivity at $T_c = 0.9$ K (under 1.2 GPa) for $X = PF_6$, $T_c = 1.1$ K (under 1.2 GPa)

for $X = AsF_6$ and $T_c = 0.38$ K (under 1.05 GPa) for $X = SbF_6$ complexes. The TMTTF compounds with $X = PF_6$, AsF_6, SbF_6 are known to show spin-Peierls (sP) transition and that with $X = Br$ has an antiferromagnetic ground state. In the case of $(TMTTF)_2PF_6$, the ground state is converted to a superconductive one with $T_c = 1.8$ K under 5.4 GPa, and $(TMTTF)_2SbF_6$ shows $T_c = 2.6$ K under 6.1 GPa. The sequential appearance of AF, sP, AF, SDW, SC and metallic phases with increasing pressure gives a fascinating physics related to the quasi-1D, electron correlations and electron–phonon coupling effect.[4,23] In addition to the Peierls instability in quasi-1D system, the dimerization of donor molecules produces Mott–Hubbard instability in metallic state and the intersite Coulomb energy V works to produce a kind of CO instability coupled with low-energy phonons in the TMTSF/TMTTF system.[23]

Thermodynamic work on TMTSF system was performed by Garoche *et al.* for ambient-pressure superconductor $(TMTSF)_2ClO_4$ in 1982.[24,25] They glued several pieces of aligned single crystals with total weight of 3.2 mg on a sapphire plate and measured heat capacity by AC technique with a frequency of 8 Hz. A thermal anomaly related to the superconductive transition was observed by them. The data obtained in this paper included those obtained under magnetic fields applied parallel to c^*-axis, which is perpendicular to the highest conductive axis (a-axis). This direction has lowest critical fields and magnetic fields sensitively affecting on the heat capacity peak in C_pT^{-1} versus T plot. They also reported that difference of cooling rates affects on the volume of superconductive electrons. In this complex, the anion ordering occurs at 24 K and the cooling process through this temperature affects on the homogeneity of low-temperature superconductive phase. The relaxed state which was attained by cooling down the sample slower than 0.1 $K \cdot min^{-1}$ from 40 K to 0.1 K showed a sharp peak, while that in the quenched state measured after cooling down the sample with a rate of 10 $K \cdot min^{-1}$ showed a broader and smaller thermal anomaly. The reduction of transition temperature was found to be 0.9 K and the heat capacity jump reduces by 22–24% in the rapidly cooled sample. We show in Fig. 3 the cooling rate dependence of the heat capacity of this compound. Through the analysis reported by Garoche *et al.* in Ref. 25 and the one by Brusetti in 1983,[26] the low-temperature thermodynamic parameters are evaluated as $\gamma = 10.5 \pm 0.5$ mJ·K^{-2}·mol^{-1} and $\beta = 11.5 \pm 0.5$ mJ·K^{-4}·mol^{-1}. The β-value is corresponding to the Debye temperature of 213 ± 3 K. Using the electronic heat capacity coefficient γ, magnitude of $\Delta C_p/\gamma T_c$ is evaluated as 1.67, which is in the strong coupling region of Bardeen–Cooper–Schrieffer (BCS) theory. More recently, possibility of unconventional pairing with the node gap for this complex is suggested by NMR experiments and existence of nodes in the superconductive gap in low-temperature heat capacity is suggested by angle-resolved heat capacity measurements by Yonezawa *et al.*[27]

In the paper of Brusetti *et al.*,[26] possible appearance of phase transition to a new field-induced phase around 1.4 K was suggested under magnetic field of 6.3 T. They

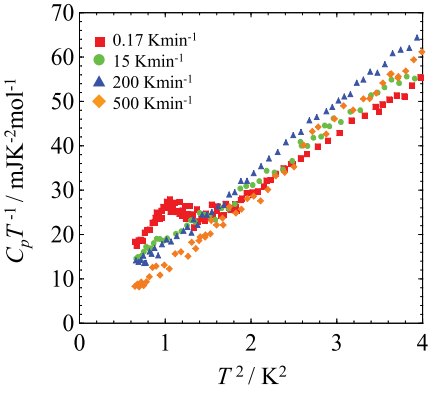

Fig. 3. (Color online) The cooling rate dependences of the C_pT^{-1} anomaly of the superconductive transition of quasi-1D superconductor, $(TMTSF)_2ClO_4$, from slow cooling of 0.17 $K \cdot min^{-1}$ to quite rapid cooling of 500 $K \cdot min^{-1}$. The distinct peak changes to the smaller one with lower T_c in the case of 15 $K \cdot min^{-1}$ and disappears in the rapid cooling higher than 200 $K \cdot min^{-1}$.[34]

speculated that the SDW phase like $(TMTSF)_2PF_6$ may be induced by applying magnetic fields. Detailed thermodynamic data of the field-induced SDW (FISDW) phase were reported by Garoche co-workers in 1986.[28,29] They reported the magnetic field dependence of AC heat capacity obtained by single-crystal sample at several temperatures. By applying magnetic field higher than 3.5 T, they found that normal metallic state changes to a semimetallic phase accompanied by sequential appearance of field-induced phase transitions. They studied the thermodynamic properties in more detail by changing magnetic fields and temperatures and constructed an H–T phase diagram where magnetic field-induced SDW phases appear. They also indicated that temperature dependence of ΔC_pT^{-1} under magnetic field differs from BCS peak shape at 10 T, while that in lower magnetic field of 5.75 T shows a mean-field-type peak.[29] The thermodynamic measurements by magnetic field sweeping were also performed by Konoike *et al.* in the dilution temperature region and they obtained cascade-type phase diagram.[30] They indicated the existence of reentrant regions around 3.3, 4.0 and 4.8 T from a density plot of second derivatives of heat capacity curvatures in subphases with even index number. The formation of superlattice structure due to anion ordering should be taken into account to explain this phenomenon. The thermodynamic properties in higher magnetic fields than those reported in Refs. 28 and 29 were studied by Fortune *et al.*[31] They observed that large heat capacity peak exists around 8 T in the magnetic sweeping curve at 0.78 K. Above this field, the field-induced SDW state assigned with a quantum number $v = 1$ retained up to higher magnetic fields until another kind of anomalous behavior with hysteresis appears above 25 T. Uji *et al.* quite recently extended the measurements up to 35 T and reported that this SDW phase is replaced by another SDW phase through a first-order transition.[19] They also investigated the rapid oscillation of C_pT^{-1} observed at high magnetic region in both papers[28,29] and concluded that they can be explained by a density of states oscillation. In 2000,

Yang *et al.* performed a systematic work in $(TMTSF)_2ClO_4$ with varying cooling rate.[32] They analyzed lattice heat capacities in slowly cooled samples and quenched samples which have SDW ground state with $T_c = 4.5$ K and performed comparative discussion. The slowly cooled sample has $\gamma = 11.5 \pm 1.0\ \text{mJ} \cdot \text{K}^{-2} \cdot \text{mol}^{-1}$ and $\beta = 10.9 \pm 0.3\ \text{mJ} \cdot \text{K}^{-4} \cdot \text{mol}^{-1}$ ($\Theta_D = 205 \pm 2$ K) while the quenched sample has $\gamma = 0\ \text{mJ} \cdot \text{K}^{-2} \cdot \text{mol}^{-1}$ and $\beta = 12.8 \pm 0.3\ \text{mJ} \cdot \text{K}^{-4} \cdot \text{mol}^{-1}$ ($\Theta_D = 216 \pm 3$ K).

TMTSF compounds which have tetrahedral anions, such as ClO_4^-, ReO_4^- and FSO_3^-, have an orientational ordering of anion sites at 24, 180 and 86 K, respectively. In these series complexes, the dynamic properties at molecular levels also affect on the electronic properties as we have mentioned in superconductive transition in $(TMTSF)_2ClO_4$ case. Thermodynamic measurements from the standpoints of such molecular dynamics are also important target of TMTCF systems.[32,33] The thermal anomaly related to the anion ordering in $(TMTSF)_2ClO_4$ has a sharp peak whose entropy estimated between 16 K and 28 K is $R\ln(4/3)$. This entropy is smaller than $R\ln 2$ corresponding to two stable conformations in the crystal. The temperature dependence of the thermal anomaly related to this anion ordering is shown in Fig. 4. A glass-like freezing of the conformation may be suggested from the peak shape of the heat capacity of the anion ordering of $(TMTSF)_2ClO_4$.[34] The anion ordering transitions of ReO_4 and BF_4 occuring at higher temperature region were reported in Ref. 35. The transition is sluggish and has hysteresis in the case of BF_4 anion, while that of ReO_4 is sharp and has weakly first-order character. However, the entropy of ReO_4 complex is smaller than $R\ln 2$ and sample dependence was also reported in Ref. 35.

The heat capacity measurements on the SDW transition of $(TMTSF)_2PF_6$ were reported by Coroneus *et al.* using AC calorimetry for a set of needle crystals (4–5 crystals) with 2.7–4.0 mg mass for the first time.[36] A thermal anomaly in temperature dependence of heat capacity was observed around 12.1 K. They

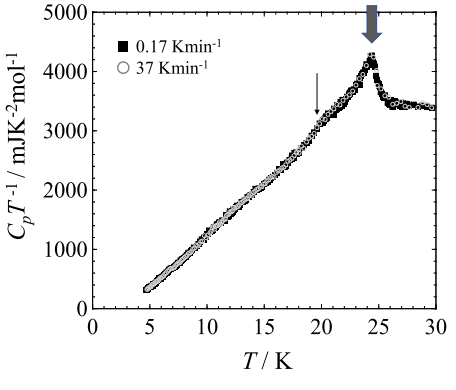

Fig. 4. The thermal anomaly in C_pT^{-1} owing to the orientation ordering of the anions in $(TMTSF)_2ClO_4$. The bold arrow indicates the transition temperature. The evaluated entropy of the anomaly is less than $R\ln 2$ and glass-like freezing may be occurring around the lower temperature side of the peak as indicated by the thin arrow.[34]

reported that the magnitude of ΔC_p for the SDW formation was less than 1% of the total heat capacity at 12 K, but has relatively narrow transition width of about 0.3 K. The analysis based on Ginzburg criterion defined by the parameter $\zeta_T = 1/(\xi_a\xi_b\xi_c\Delta C_p)^2$, where ξ_a, ξ_b and ξ_c are correlation lengths and ΔC_p is a heat capacity jump at the transition, was performed in the paper. ζ_T was roughly 50 times larger than the thermal anomaly associated with field-induced SDW transition in $(TMTSF)_2ClO_4$, demonstrating that the SDW in this system has long-range nature. The magnetic field of 7.2 T does not change the peak shape which is also in contrast with the behaviors of FISDW in $(TMTSF)_2ClO_4$. Similar peak shape related to the thermal anomaly whose ΔC_p corresponds to 1.5% of C_p is observed by Odin *et al.* obtained by the quasi-adiabatic method.[37] Powell *et al.* reported that the peak shape of SDW transition is very sensitive to residual disorders by comparing the single-crystal AC calorimetry result with that of pellet sample and quasi-adiabatic measurements. The peak observed in single crystal disappears in the pelletized sample, which is sometimes observed in organic charge transfer systems.[38]

Low-temperature thermodynamic properties in the SDW state have dynamical characters which are essential for this system. Coexistence of various kinds of interactions produces complicated coupling of charges, lattices and spin degrees of freedom and causes nonequilibrium freezing at low temperatures. These dynamics are dominated by long relaxation time in the order of 10^{0-3} s which is extraordinarily longer as those in the electronically ordered states. Heat capacity measurements for these low-energy states were studied thoroughly by Lasjaunias and co-workers by the usage of semiadiabatic, relaxation and transient-pulse techniques. At first, they performed low-temperature heat capacity measurement of $(TMTSF)_2PF_6$ down to 0.15 K in Ref. 39. They reported that the heat capacity of $(TMTSF)_2PF_6$ reveals T^3 term plus T-linear term in a temperature range below 2.9 K. The β-value is $14.5 \pm 0.5\ \mathrm{mJ \cdot K^{-4} \cdot mol^{-1}}$. It is more accurately reported in Ref. 35 that the low-temperature phonon contribution to the heat capacity obeys T^3 law only in the restricted temperature region below about 3 K and existence of very broad bump structure in C_pT^{-3} versus T plot is observed as a common feature of TMTSF system. The bump is attributed to low-energy phonons related with a librational motion of sacked donors and should be explained using Einstein modes.

In Ref. 39, Lasjaunias *et al.* observed a small discontinuity around 3.5 K in the temperature dependence of heat capacity, which is interpreted as a transformation to subphase related to the SDW state. In the paper of Odin *et al.*,[37] this anomaly was reported to be accompanied by a kind of kinetic properties. They reported that if the equilibrium heat capacity was measured using the adiabatic method, the β-values are 18.5–19 $\mathrm{mJ \cdot K^{-4} \cdot mol^{-1}}$, while for a kind of dynamic measurements like transient-pulse technique, β decreases to about $14.5 \pm 0.5\ \mathrm{mJ \cdot K^{-4} \cdot mol^{-1}}$. The nonexponential enthalpy relaxation was also observed in the subsequent report by Biljaković *et al.*[40] This gives a strong evidence for the glass formation at low temperatures. The indication of phenomenological analogy in the molecular glass system

was also supported by an existence of aging effects and clear cooling rate dependence which were studied in various conditions in Ref. 41. A frequency-dependent peak in the dielectric constant ε' was observed by Lasjaunias *et al.* which also indicated the formation of glass state in SDW state. Similar step-like anomaly accompanied by hysteretic behavior is reported in $(TMTSF)_2AsF_6$ system in the SDW state.[42]

Another important point suggested by the same group is a time-dependent phenomenon in thermodynamic properties at extremely low temperatures.[43–48] Lasjaunias *et al.* observed that the SDW state of $(TMTSF)_2PF_6$ system has an unexpectedly long relaxation time, which is affected by an aging process.[42,43] They indicated that the relaxation time distributes in wide timescale. Therefore, heat capacity values show differences depending on the timescale used for the data analyses. They reported that similar time-dependent behaviors are also observable in SDW state of $(TMTSF)_2AsF_6$.[42] Later, the commensurate AF system of $(TMTTF)_2Br$[46,47] and $(TMTTF)_2PF_6$ with a spin-Peierls ground state were also found to have similar dynamic characters. In 2002, Lasjaunias *et al.* extended the heat capacity measurements down to 30 mK for $(TMTTF)_2Br$ and $(TMTTF)_2PF_6$ and confirmed that the low-energy excitations in these ordered ground states have a glassy character with strongly time-dependent behavior.[48] They estimated that heat capacity determined by nearly equilibrium situation may have large Schottky contribution, while the data obtained by transient-pulse technique gives reduced heat capacity values. They obey T^{-2} Schottky terms representing low-energy excitations. The behavior resembles the low-energy excitations in DW state, although they have commensurate magnetic structure. In this complex, dimerization of donors produces a kind of Mott–Hubbard localization. However, the existence of intersite Coulomb interaction V tends to make CO fluctuations which are probed as anomalous behavior in dielectric properties. The glass-like behavior observed in lattice heat capacity is considered to be related to these CO structures. Strong electron–lattice coupling with slow dynamics characteristic of intersite Coulomb interaction is considered as the origin of such glass-like electronic states in crystals with regular periodic lattices.

These peculiar lattice dynamics reported by Lasjaunias *et al.*[39–48] may be related to the results reported by other groups. The large hysteretic behavior was observed in thermopower measurements by Bondarenko *et al.* and was discussed in relation to the random pinning in the SDW state in Ref. 49. A hump in field dependences in heat capacity of $(TMTSF)_2AsF_6$ system is reported by Yamaguchi *et al.*, which has been discussed in relation to magnetoresistance in the SDW state.[50] The low-temperature thermodynamic behavior of $(TMTCF)_2X$ system is a subject to be further pursued over wide timescale.

The nature of low-energy excitations in the ground state has been further investigated by Mélin *et al.* in $(TMTTF)_2Br$ complex.[51] This complex has large LEEs but this complex has a narrow spectrum of relaxation times due to the commensurate magnetic ordering. They evaluated the equilibrium heat capacity at extremely low-temperature region and observed that it obeys T^{-2} terms explained by the high-temperature tail of Schottky heat capacity. They reported that this T^{-2} term

depends on magnetic fields. The similar analysis of heat capacity data under magnetic fields was performed by them and systematic increase of the coefficient of T^{-2} term by magnetic fields was demonstrated. They explained that the excitations in the magnetic fields have different character from zero fields which is explained by the existence of strong-pinning impurities. The variation of the magnitude of the Schottky heat capacity with H^2 means the deconfinement of soliton–antisoliton pairs triggered by Zeeman coupling of spin degrees of freedom created by different pinning centers as explained by Sahling *et al.*[52] in 2007 and Biljaković *et al.*[53]

The heat capacity measurements of spin-Peierls transitions in the low-pressure region of the universal phase diagram have not been detected until recently. In $(TMTTF)_2AsF_6$ which has a transition temperature of $T_{sP} = 11$ K, de Souza *et al.* have measured the heat capacity and observed a broad anomaly. The shape of the heat capacity heat has been discussed in comparison with that of thermal expansion measurements by them.[54] According to their report, there is no anomaly in $(TMTTF)_2PF_6$ with lower sP transition temperature. The short-range nature related to the charge and lattice degrees of freedom is suggested in this complex.

3. Thermodynamic Properties of κ-(BEDT-TTF)$_2X$ System

It is well known that BEDT-TTF-based charge transfer compounds with κ-type structure show interesting physical characters produced by electron correlations in the 2D bands.[55–58] The Mott insulating complexes with antiferromagnetic transitions around 10–30 K, nonordered magnetic complexes such as spin-liquid systems, metallic and superconductive complexes with relatively high transition temperatures are realized in this structure depending on the difference of the electron correlation parameter and the frustration parameter. Understanding the origins and relations between these states from unified viewpoint is an important subject for organic conductors. As we have mentioned in Sec. 2, the important parameters which determine electronic properties are onsite Coulomb interaction U and bandwidth W. The κ-type structure is known as a rigidly dimerized structure. Donor dimers with face to face contact are arranged in nearly orthogonal position and consequently a zigzag network structure is constructed.[55–57] The intradimer transfer energy is usually larger than other transfers and therefore each dimer is considered as a structural unit in the 2D plane. There are roughly two types of transfer energies, t and t', between neighboring dimers as shown in Fig. 5. Usually, t is larger than t' ($t > t'$) and the κ-type arrangement is considered as a square lattice of the dimer unit in this case. If the transverse transfer between dimers t' is comparable with t ($t \approx t'$), the dimer lattice is considered as a triangular lattice which is discussed from the viewpoint of frustration physics.

The rigid dimerization characteristic in this κ-type structure leads the electronic structure of these compounds to a unique situation. Since each dimer is considered as a structural unit in this arrangement, the electronic state is interpreted as effectively half-filled and simple Mott–Hubbard physics determined by competition

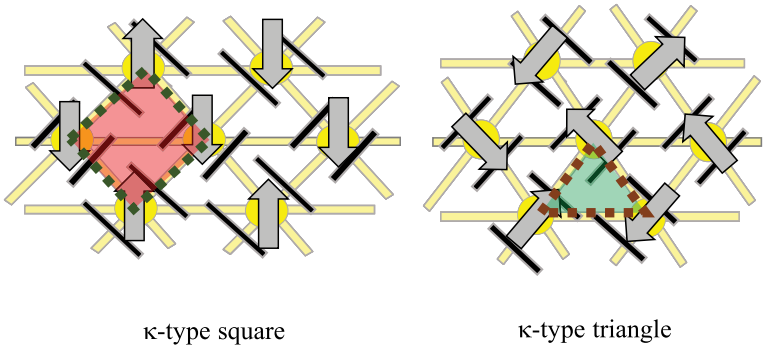

Fig. 5. (Color online) The schematic view of the relation of the dimer arrangement in the κ-type structure. Depending on the magnitude of the interdimer transfer, the κ-type structure is considered as a square lattice or a triangular lattice.

of the onsite (on-dimer) interaction U and bandwidth W appears. When U is larger than W, the system becomes a Mott insulating state with antiferromagnetic ground state. The compounds with square and rectangular dimer lattice structures show antiferromagnetic ordering, while the triangular lattice system like κ-(BEDT-TTF)$_2$Cu$_2$(CN)$_3$ has a gapless spin-liquid ground state. On the other hand, in the region where W exceeds U, the ground state would be a strongly correlated metallic state. The superconductivity with relatively high-T_c ($\approx$10 K) appears in this region. The pressure–temperature phase diagram shown in Fig. 6 in which the antiferromagnetic phase is neighboring to the superconducting phase is established by Kanoda and co-workers[55–58] These two states can be tuned by external or chemical

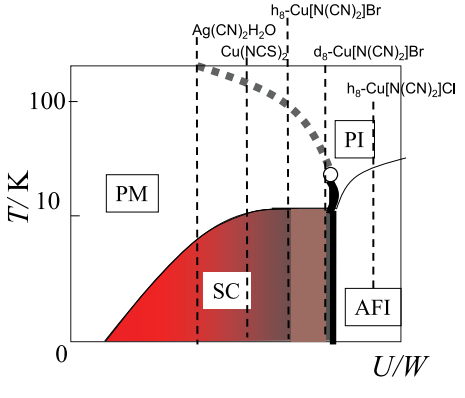

Fig. 6. (Color online) The conceptual phase diagram of dimer-Mott-type organic compounds. The dashed lines in the phase diagram indicate the position of the several κ-type (BEDT-TTF)$_2X$ compounds with different sizes of X [X = Ag(CN)$_2$H$_2$O, Cu(NCS)$_2$, Cu[N(CN)$_2$]Br, Cu[N(CN)$_2$]Cl]. The difference of the BEDT-TTF molecules whose ethylene groups are hydrogen (h$_8$) and deuterium (d$_8$) also works as chemical pressure effect for the latter two and it is also marked in the phase diagram. PM, PI, SC and AFI denote paramagnetic metal, paramagnetic insulator, superconductor and antiferromagnetic insulator, respectively.[55–58]

pressures. The superconductive compounds in κ-type structure are known to possess relatively high transition temperature as is realized in κ-(BEDT-TTF)$_2$Cu(NCS)$_2$ ($T_c = 10.4$ K) and κ-(BEDT-TTF)$_2$Cu[N(CN)$_2$]Br ($T_c = 11.6$ K). The heat capacity measurements on these complexes have been performed by many groups with the purpose of clarifying the electronic structure in the phase diagram and also unveiling the origin and character of high-T_c superconductivity in organics. In the following, we survey low-temperature heat capacity works of insulating and metallic compounds with κ-type complexes focusing on the electronic states and phase diagram. The details of thermodynamic works on the superconductivity of several compounds with κ-type structure are introduced in the latter part.

The electron correlations induced by the onsite Coulomb repulsion in dimer unit $U_{\rm dimer}$ are expressed as $2t_{\rm dimer}$ in the dimer approximation as discussed by Kanoda *et al.*[55–58] Although the superconductive transition temperatures of these compounds are relatively high, the γ-values are almost similar to those of nonsuperconducting conductors and low-T_c superconductor, for example α-(BEDT-TTF)$_2$NH$_4$Hg(SCN)$_4$ and other organic conductors (DMe-DCNQI)$_2$Cu. There are some exceptions like κ_L-(BEDT-TTF)$_2$Ag(CF$_3$)$_4$TCE and κ-(BEDT-TTF)$_4$Hg$_{3-\delta}X_8$. This situation is similar to the case of high-T_c cuprates in that antiferromagnetic spin fluctuations are detected for example by ^{13}C-NMR as a large enhancement of $(T_1T)^{-1}$, but the electronic heat capacity coefficient is not much enhanced as compared with enhanced metallic systems of d- or f-electron metals. The thermodynamic measurements on κ-type compounds were performed by Andraka and co-workers by thermal relaxation technique in the initial stage. The γ-value of 10 K-class superconductive complex of κ-(BEDT-TTF)$_2$Cu(NCS)$_2$ is 22 ± 3 mJ $\cdot$ K^{-2} $\cdot$ mol^{-1} as mentioned by Andraka *et al.*[59] and that of κ-(BEDT-TTF)$_2$Cu[N(CN)$_2$]Br is 25 mJ $\cdot$ K^{-2} $\cdot$ mol^{-1} in the initial stage of investigation.[60]

To establish the 2D dimer-Mott picture reported by Kanoda *et al.*,[55,56] characterization of the insulating phase by heat capacity measurements was performed in 1996.[7,8] In this series of publications, the Mott insulator samples of κ-(BEDT-TTF)$_2$Cu[N(CN)$_2$]Cl and deuterated κ-(d$_8$:BEDT-TTF)$_2$Cu[N(CN)$_2$]Br in which eight hydrogen atoms in ethylene group of h$_8$:BEDT-TTF complex have been deuterated, were studied. Although the pristine compound κ-(BEDT-TTF)$_2$Cu[N(CN)$_2$]Br is a superconductor with $T_c = 11.4$ K, the deuterated compound shifts to the antiferromagnetic region due to a chemical pressure effect. The low-temperature heat capacities of κ-(BEDT-TTF)$_2$Cu[N(CN)$_2$]Cl and κ-(d$_8$:BEDT-TTF)$_2$Cu[N(CN)$_2$]Br clearly show vanishing γ-term in C_pT^{-1} versus T^2 plot. The magnetic fields up to 8 T do not change the heat capacity in the insulating sample. The opening of charge gap at the Fermi energy even though the band filling is effectively half-filled supports the picture that the dimer-Mott system with localized spins and the electron localization by impurities or disorders to make insulating state are excludible. Another important point reported in this work is the absence of thermal anomaly in the Néel temperatures in both compounds. The effective $J = 2t^2/U_{\rm dimer}$ in this system is evaluated as 200–250 K and a large

amount of magnetic entropy by short-range correlations exists at higher temperatures. Furthermore, quantum fluctuations in the Mott insulating state obscure the long-range nature of phase transitions. There is an absence of thermal anomaly around the Néel temperatures in κ-(BEDT-TTF)$_2$Cu[N(CN)$_2$]Cl and similarly in the dimerized complex of β'-(BEDT-TTF)$_2$ICl$_2$ system.[61,62] The latter compound is also a Mott insulating system which does not show any γ-value and relatively hard lattice expressed by smaller $\beta = 7.46\ \mathrm{mJ \cdot K^{-4} \cdot mol^{-1}}$. This compound was found to convert to 14.6 K superconductor under the strong pressure of about 80 GPa as observed by Taniguchi *et al.* in 2003.[63] Although the Mott insulating picture was certainly a good approximation for these κ-type compounds with strong U, the internal degrees of freedom in the dimer unit and intermolecular Coulomb interaction V have recently been investigated to give charge disproportionation in the κ-type and β'-type compounds by optical experiments.

It is also important to mention here that the cooling rates influence the physical properties. The nature of superconductivity of κ-(BEDT-TTF)$_2$Cu[N(CN)$_2$]Br and its deuterated complex is affected by disorders produced by the rapid cooling process from room temperature down to liquid He temperature. Since the deuterated sample is located just close to the boundary, the drastic change in charge-transport properties, for example, the insulator to superconductive transition, occurs by controlling the cooling rate.[64] This phenomenon is considered as a kind of volume effect specific for Mott–Hubbard system where metallic and antiferromagnetic insulating phases are neighboring by a first-order phase boundary. Akutsu *et al.* performed high-resolution AC heat capacity measurements of κ-(BEDT-TTF)$_2$Cu[N(CN)$_2$]Br and observed that hump structure indicative of a glass-like anomaly around 90 K exists in temperature dependence with a frequency of 0.24 Hz.[65] They also studied frequency dependence and found that the hump structure broadens gradually and shifts to higher temperature with increasing frequencies. The hump structure shifts to about 105 K at 1 Hz and to 110 K at 4 Hz. Their group concluded that the ethylene groups at the edge of BEDT-TTF molecules have two stable conformations and glass-like freezing occurs during the cooling process. Analyzing the frequency dependence of the AC heat capacity, the glass formation temperature in the static limit is consistent with the temperature where resistivity and thermal expansion show anomalies ($T_g = 77$ K). Similar glass-like freezing is also observed in κ-(BEDT-TTF)$_2$Cu[N(CN)$_2$]Cl and in (DMET)$_2$BF$_4$, (DMET)$_2$ClO$_4$ and (DIMET)$_2$BF$_4$ with nonsymmetric donor molecules.[66]

In order to investigate thermodynamic nature around the boundary region of superconductive phase and insulating phase, the low-temperature thermodynamic measurements were performed by Nakazawa and Kanoda with different cooling rates between 0.07 $\mathrm{K \cdot min^{-1}}$ and 1.7 $\mathrm{K \cdot min^{-1}}$ for d_8 sample.[67] The γ-value changes from $0.65 \pm 0.36\ \mathrm{mJ \cdot K^{-2} \cdot mol^{-1}}$ for $0.07\ \mathrm{K \cdot min^{-1}}$ to $0.73 \pm 0.47\ \mathrm{mJ \cdot K^{-2} \cdot mol^{-1}}$ for $1.7\ \mathrm{K \cdot min^{-1}}$ and β value in both cooling rates is $11.3\ \mathrm{mJ \cdot K^{-4} \cdot mol^{-1}}$, meaning that a slight change of electronic heat capacity occurs in the thermodynamic sense. The sample that experienced an annealing process around the liquid nitrogen

temperature shows slight increase of $\gamma = 1\ \mathrm{mJ \cdot K^{-2} \cdot mol^{-1}}$ which means that the conducting component in κ-(d_8:BEDT-TTF)$_2$Cu[N(CN)$_2$]Br is partial and exists like a filament in the thermodynamic sense. More recently, partial deuterated samples of κ-(BEDT-TTF)$_2$Cu[N(CN)$_2$]Br were investigated and even in the superconductive state with almost similar T_c, density of states decreases with increasing the deuteron numbers. For example d_4 samples described as d[2,2], which means two hydrogen atoms in each ethylene group on both sides of BEDT-TTF have been deuterated as shown in Fig. 7, show 9–10 $\mathrm{mJ \cdot K^{-2} \cdot mol^{-1}}$. The d_2 with d[1,1] that means one hydrogen atom in each ethylene group has been deuterated, has nearly 20 $\mathrm{mJ \cdot K^{-2} \cdot mol^{-1}}$.[68,69] The decrease of γ-value by approaching from the superconductive

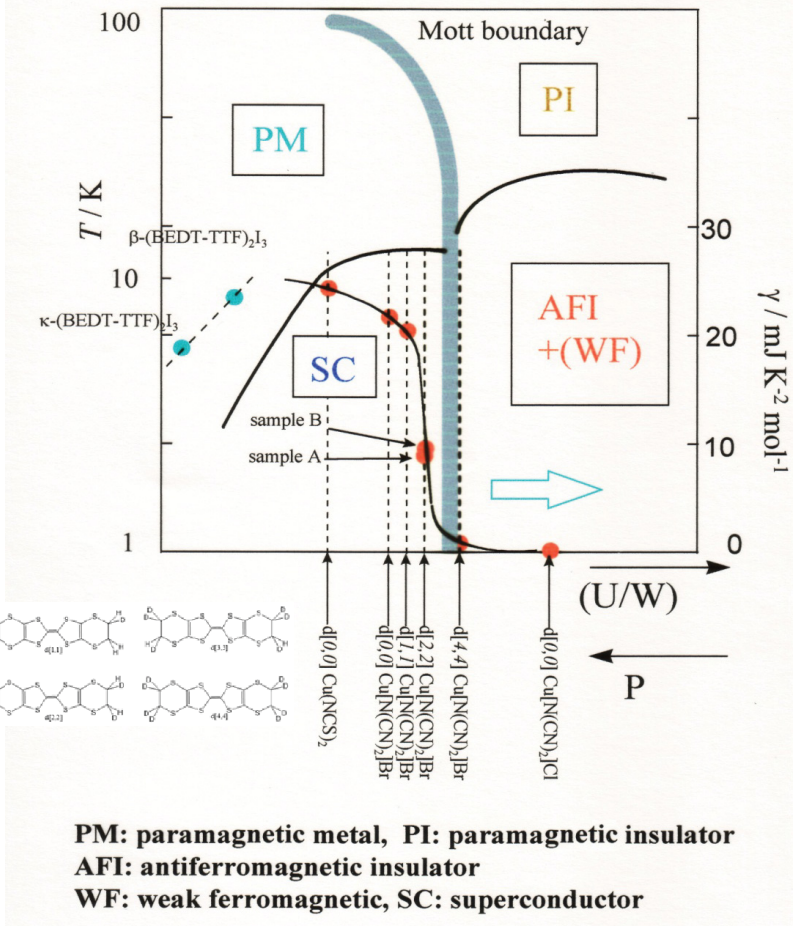

Fig. 7. (Color online) The variations of the normal state electronic heat capacity coefficient γ in the superconductive phase are shown with the phase diagram. The partial deuteration of BEDT-TTF as shown in the figure can tune the electronic state near the Mott boundary between the superconductive phase and the antiferromagnetic insulator phase.[68,69]

region to antiferromagnetic insulating region in the phase diagram, was studied by Taylor *et al.* in Ref. 70 by controlling the cooling rate across the glass temperatures. They controlled the cooling rate between 80 K and 65 K through the glass transition at $T_g = 77$ K and measured heat capacity in rapidly cooled sample. They observed that the cooling slower than 20 $\mathrm{K} \cdot \mathrm{min}^{-1}$ causes a bulk superconductivity but the γ-value obtained under magnetic fields gradually decreases. At 53 $\mathrm{K} \cdot \mathrm{min}^{-1}$, they observed that the γ decreases down to about 1/2 of the original value, although the decrease of T_c itself is only 0.4 K. The drastic decreases of γ in rapidly cooled κ-(BEDT-TTF)$_2$Cu[N(CN)$_2$]Br can be interpreted as a kind of phase separation of superconductive region and antiferromagnetic insulator region inevitably produced around the first-order phase transition in Mott insulator and metallic system.

Apart from the discussion of universal phase diagram of κ-(BEDT-TTF)$_2X$ system, we should consider a unique system which is understood as a hole-doped system in effectively half-filled state. Oike *et al.*[71] have reported the anomalous properties of nonstoichiometric complexes of κ-(BEDT-TTF)$_4$Hg$_{2.89}$Br$_8$ (Br complex) and κ-(BEDT-TTF)$_4$Hg$_{2.78}$Cl$_8$ (Cl complex) of which Hg chain structure in the anion layer has an incommensurate structure with 2D BEDT-TTF structure as reported by Lyubovskaya *et al.*[72] Since the Hg ions in the chain are divalent, the averaged hole number in donor layers is shifted by 10% for Br complex and 18% for the Cl complex from the half-filled state. They observed that antiferromagnetic fluctuations were enhanced (as were detected by T_1^{-1}). The heat capacity measurements were performed by Naito *et al.* and estimation of γ-terms was performed.[73,74] The curious low-energy phonon background in C_p dominated by heavy elements of Hg has been evaluated by Tarasov's model and they reported that the γ-value of Br complex is 55 $\mathrm{mJ} \cdot \mathrm{K}^{-2} \cdot \mathrm{mol}^{-1}$ and that of Cl complex is 52 $\mathrm{mJ} \cdot \mathrm{K}^{-2} \cdot \mathrm{mol}^{-1}$. This value is nearly twice as large as other conducting complexes. In the case of Cl complex, temperature dependences of heat capacity resemble to those of heavy electron systems. The superconductive transition of the Br complex was also studied by Naito *et al.*[73] and Yamashita *et al.*[75] and very broad peak with $\Delta C_p T^{-1} = 30$ $\mathrm{mJ} \cdot \mathrm{K}^{-2} \cdot \mathrm{mol}^{-1}$ was observed. Yamashita *et al.* reported that the cooling rate from room temperature to liquid helium temperature affects on the superconducting volume fraction estimated from the heat capacity jump around T_c.

The thermodynamic researches on 10 K-class superconductors in the κ-type complex have been conducted for about 30 years and attracting the interests of both theorists and experimentalists in the field of organic compounds, because this subject has common aspects with d-electron systems such as high-T_c cuprates and f-electron systems. The heat capacity measurements around T_c of κ-type organic superconductors were performed mainly by thermal relaxation calorimetry and also by high-resolution AC calorimetry technique. The heat capacity measurements of superconductive transition of κ-(BEDT-TTF)$_2$Cu(NCS)$_2$ system were performed by Katsumoto *et al.* in 1988 by AC technique.[76] They observed that a broad heat capacity anomaly related to the superconductive transition exists around

9 K. The estimation of γ obtained by extrapolation of high-temperature data was 5 $\mathrm{mJ \cdot K^{-2} \cdot mol^{-1}}$ and Debye temperature was 175 K. Since the temperature region of their experiment is above 3 K, these data contain ambiguity. Andraka *et al.* in 1989 reported that $\Delta C_p T^{-1}$ is larger than 50 $\mathrm{mJ \cdot K^{-2} \cdot mol^{-1}}$ in Ref. 59. Graebner *et al.* developed a new high-resolution AC technique called as modulation bath AC technique which is available for tiny sample measurements.[77] They used typically 0.2 mg single crystals and observed a clear anomaly related to superconductive phase transition. They also published the data obtained under in-plane and out-of-plane magnetic fields. The structure of the peaks resembles to that observed by Katsumoto *et al.* From the data at 0 T, Graebner *et al.* estimated that $\Delta C_p/\gamma T_c = 1.5 \pm 0.15$ using $\gamma = 34$ $\mathrm{mJ \cdot K^{-2} \cdot mol^{-1}}$ estimated from Pauli susceptibility value. This γ contains ambiguity and seems to be overestimated with a factor of about 1.5 as compared with the data from other works directly measured by low-temperature heat capacity. The heat capacity peak reported by them suggests that this compound is in the region of strong coupling. They also determined the H_{c2} versus T relation from heat capacity data that gives $-dH_{c2}/dT = 16$ T/K in the $H_{\|}$ plane direction and $-dH_{c2}/dT = 0.75$ T/K in the $H_{\perp}$ plane direction. Two-dimensional nature of the layered organic superconductor was suggested thermodynamically. The low-temperature heat capacity of κ-(BEDT-TTF)$_2$Cu(NCS)$_2$ by relaxation calorimetry with absolute precision was measured by Andraka *et al.* in 1989.[59] From the $C_p T^{-1}$ versus T^2 plot of low-temperature heat capacity measured under magnetic field up to 12.5 T, they estimated that the normal state γ-value is 25 ± 3 $\mathrm{mJ \cdot K^{-2} \cdot mol^{-1}}$. By combining these two data, they claimed that the superconductivity is in strong coupling region with $\Delta C_p/\gamma T_c > 2$ and reaches to about 2.8 if the mean-field approximation is applied by conserving the entropy.

In the case of κ-(BEDT-TTF)$_2$Cu[N(CN)$_2$]Br complex, Andraka *et al.* also performed heat capacity measurements by relaxation calorimetry. They also measured heat capacity up to 14 T and obtained that the normal state γ-value estimated from $C_p T^{-1}$ versus T^2 plot is equal to $\gamma = 22 \pm 3$ $\mathrm{mJ \cdot K^{-2} \cdot mol^{-1}}$ and the Debye temperature equals 210 K. They also estimated $\Delta C_p/\gamma T_c = 2 \pm 0.5$, which is comparable with the data of κ-(BEDT-TTF)$_2$Cu(NCS)$_2$.[60] Although there are sample dependences in the reported γ-values, the value of κ-(BEDT-TTF)$_2$Cu[N(CN)$_2$]Br is smaller than those reported in κ-(BEDT-TTF)$_2$Cu(NCS)$_2$ in spite of higher transition temperature. The coupling strength of the electron pairs appearing in the condensation energy seems to be larger in the former, since it is located in the boundary region of the phase diagram.

Thermodynamic data on the middle class T_c compound κ-(BEDT-TTF)$_2$I$_3$ with transition temperature of 3.4 K was reported by Wosnitza *et al.* using a high-resolution heat pulse technique between 0.25 K and 20 K with magnetic fields up to 6 T. They determined that $\gamma = 18.9$ $\mathrm{mJ \cdot K^{-2} \cdot mol^{-1}}$ and $\beta = 10.3 \pm 1$ $\mathrm{mJ \cdot K^{-4} \cdot mol^{-1}}$, corresponding to the Debye temperature $\Theta_D = 218 \pm 7$ K.[78,79] From the analysis of wide temperature range, they indicated that the $C_p T^{-3}$ versus T plot shows a broad peak structure due to the low-energy phonons due to

librational motions of BEDT-TTF molecules. The simple Debye T^3 terms appear only in the restricted region below about 3 K. They also observed that under magnetic fields nuclear hyperfine structure possibly by iodine and hydrogen appears even under a weak magnetic field of 0.5 T. The analysis of $\Delta C_p/\gamma T_c$ in κ-(BEDT-TTF)$_2$I$_3$ yields 1.6 ± 0.2 and they also claimed that the superconductivity is strong coupling type. The heat capacity of the compound κ-(BEDT-TTF)$_2$Ag(CN)$_2$H$_2$O with transition temperature of 5.0 K was reported by Ishikawa *et al.*[80] They measured heat capacity by relaxation technique using single crystal.[80] They observed a thermal anomaly of the superconductive transition at 5.0 K. The heat capacity peak is evaluated as $\Delta C_p/T_c = 30\ \mathrm{mJ \cdot K^{-2} \cdot mol^{-1}}$ and the electronic heat capacity coefficient γ obtained under magnetic fields up to 8 T is evaluated as 28 $\mathrm{mJ \cdot K^{-2} \cdot mol^{-1}}$. The $\Delta C_p/\gamma T_c$ is evaluated as 1.1. They reported that the residual γ_{res} in the superconductive state is 5.1 $\mathrm{mJ \cdot K^{-2} \cdot mol^{-1}}$ corresponding to about 18% of the normal state γ-value even in high-quality single crystal. The cooling rate dependence was absent in thermodynamic properties for this complex. More recent work suggests that the residual γ_{res} should be decreasing in case of the fitting by a model with nodal gap feature, although the low-temperature experiments are necessary to discuss further. Figure 8 shows the temperature dependence of electronic heat capacities of two κ-type compounds.[81]

The heat capacity of another superconductive complex of κ_L-(BEDT-TTF)$_2$Ag(CF$_3$)$_4$TCE was measured by Wosnitza *et al.*[82] between 0.3 K and 20 K by quasi-adiabatic technique. This compound has superconductive transition at 2.4 K by AC susceptibility measurements, but the heat capacity does not show

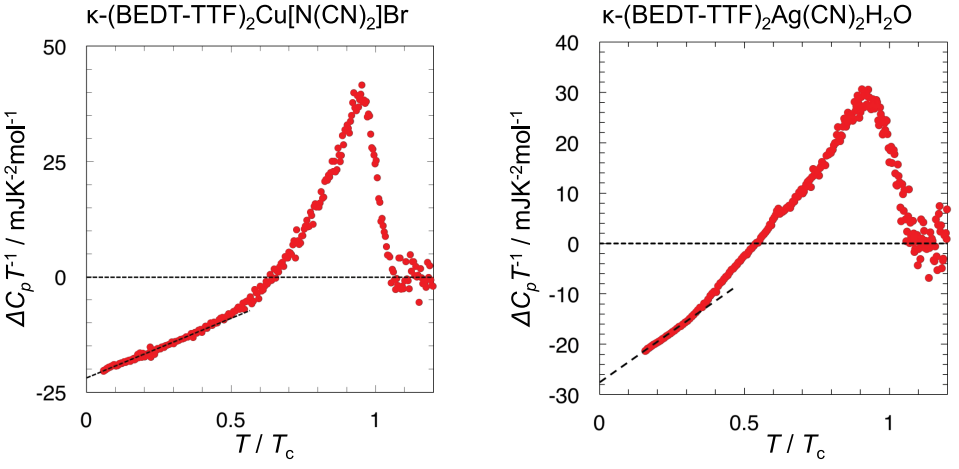

Fig. 8. (Color online) The temperature dependence of the electronic heat capacities ΔC_p determined by subtracting the normal state data obtained under magnetic fields above H_{c2} from the 0 T data for two compounds κ-(BEDT-TTF)$_2$Cu[N(CN)$_2$]Br and κ-(BEDT-TTF)$_2$Ag(CN)$_2$H$_2$O. The former has higher T_c with 11.6 K and the latter has middle class T_c of about 5 K. Both compounds show T^2 dependence at low-temperature region due to the existence of the node structure of the superconductive gaps.[81]

thermal anomaly at the corresponding temperature. The application of magnetic field of 1 T shows clear reduction of heat capacity below this temperature, which demonstrates the existence of superconductive electrons at low temperatures. The temperature dependence of heat capacity under magnetic fields was fitted by the formula: $C_p = \gamma + \beta T^3 + \delta T^5$ using the data up to 5 K and the results were obtained as $\gamma = 50\ \mathrm{mJ \cdot K^{-2} \cdot mol^{-1}}$, $\beta = 18\ \mathrm{mJ \cdot K^{-4} \cdot mol^{-1}}$ and $\delta = 1.46\ \mathrm{mJ \cdot K^{-6} \cdot mol^{-1}}$. The Debye temperature is estimated as $\Theta_D = 203 \pm 10$ K. They reported that about 50% of electrons remain as normal even at low temperatures. The origin of the γ-enhancement is not clarified, since the disorder effects in sample cannot be excluded yet.

It is important to get precise temperature dependence of electronic heat capacity which reflects the gap structure around the Fermi surface. In order to discuss this point, Nakazawa and Kanoda performed heat capacity measurements of κ-(BEDT-TTF)$_2$Cu[N(CN)$_2$]Br in dilution temperature region in 1997.[83] By comparing the data of superconductive κ-(BEDT-TTF)$_2$Cu[N(CN)$_2$]Br and insulating κ-(d$_8$:BEDT-TTF-TTF)$_2$Cu[N(CN)$_2$]Br at low temperatures, they show that the electronic heat capacity below about 3 K has a quadratic term $C_{\mathrm{el}} = \alpha T^2$ with a coefficient $\alpha = 2.2\ \mathrm{mJ \cdot K^{-3} \cdot mol^{-1}}$. They also claimed that even in the superconductive state T-linear term expressed as $\gamma_{\mathrm{res}} T$ with $\gamma_{\mathrm{res}} = 1.2\ \mathrm{mJ \cdot K^{-2} \cdot mol^{-1}}$ exists in good quality samples. The existence of this residual γ_{res} means that nearly 5% of electrons remain as normal electrons. The sample dependence of this

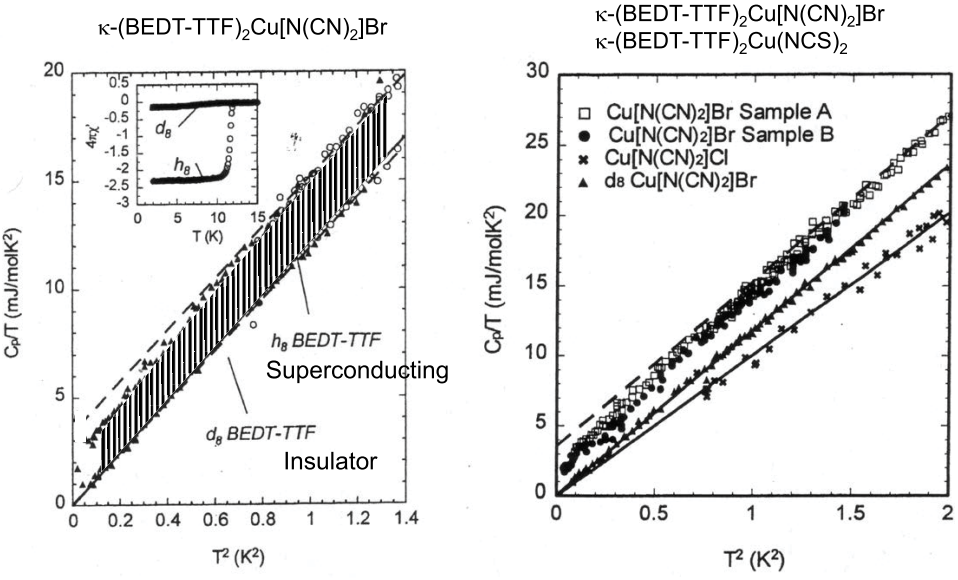

Fig. 9. The temperature dependence of the heat capacities of 10 K-class superconductive compounds κ-(BEDT-TTF)$_2X$ [X = Cu[N(CN)$_2$]Br, Cu(NCS)$_2$]. The heat capacity data of the Mott insulating compounds with X = Cu[N(CN)$_2$]Cl and the deuterated compound with X = Cu[N(CN)$_2$]Br are also shown as reference data.[83,84]

residual term was also studied. The temperature dependence of electronic heat capacity shown in Fig. 9 deviates from the BCS curve calculated by assuming a full gap with $2\Delta/k_BT_c = 3.52$. They also studied how γ recovers in the vortex state by measuring heat capacity under magnetic fields. They observed that γ obeys $\gamma = k\gamma n(H/H_{c2})^{1/2}$ where k is a coefficient of order of unity. These results demonstrate that the superconductivity is d-wave with line nodes in the cylindrical Fermi surface. Almost the same tendency was observed in κ-(BEDT-TTF)$_2$Cu(NCS)$_2$ which also has larger α and very nearly similar γ values.[84] The heat capacity results at extremely low temperature were consistent with the assertion of d-wave pairing proposed by T^3 dependence of T_1^{-1} in the superconductive state V-shape spectrum of I–V curves in tunneling spectroscopy by STM[85] and ^{13}C-NMR works.[86–88]

The discussions on the peak shape and the overall temperature dependences of electronic heat capacity have given an important prediction for gap-symmetry of the superconductivity of the dimer-Mott system. In 1998, Elsinger *et al.* have claimed that the lattice estimation using deuterated complex in low-temperature region in Ref. 83 gives rise to ambiguity for accurate discussion on electronic state.[89] They measured heat capacity of κ-(BEDT-TTF)$_2$Cu[N(CN)$_2$]Br between 1.7 K and 21 K under magnetic fields of 0 T and 14 T. They subtracted the data under magnetic fields from 0 T data and discussed the overall peak shape in this temperature range. They assumed a full gap model with extremely strong coupling region and succeeded to fit the electronic heat capacity with a model with $\alpha = 2.7$. After the work of Elsinger *et al.*, Müller *et al.* performed similar analysis on κ-(BEDT-TTF)$_2$Cu(NCS)$_2$ between 2 K and 30 K and with magnetic fields of 0 T and 8 T.[90] They also claimed that the strong coupling model holds for organic superconductors as was first predicted by Graebner *et al.*.[77] The relatively larger peak than that expected from the BCS weak coupling theory is also confirmed by Yamashita *et al.* for κ-(BEDT-TTF)$_2$Cu(NCS)$_2$ in 2005.[91]

Although the fitting by the strong coupling model is performed with the assumption of the full gap model based on BCS theory, which is inconsistent with the extremely low temperature below 2 K in Ref. 83, the subsequent work by Taylor *et al.* in 2007 derived a distinct answer for this point.[92] They measured the heat capacities of two high-quality compounds with high-resolution technique at 0 T and 14 T and analyzed the peaks by α-model which takes into account the strength of coupling. They analyzed in s-wave and d-wave cases and compared the result. Their high-resolution data even at low-temperature region clearly indicated that the low-temperature behaviors below 4–6 K can be well fitted by d-wave model with strong coupling region of $\alpha = 1.73$ and $\gamma_n = 26.6\ \mathrm{mJ \cdot K^{-2} \cdot mol^{-1}}$. The quadratic temperature dependence existing at low temperatures is consistent with Ref. 83, though the deviation from T^2 above 3 K is probably attributable to the underestimation of lattice terms. The similar result is also reported recently by Imajo *et al.* in κ-(BEDT-TTF)$_2X$ compounds.[81]

Taylor *et al.* also studied the cooling rate dependence of superconductive state for κ-(BEDT-TTF)$_2$Cu[N(CN)$_2$]Br complex in Ref. 70. They compared the

electronic heat capacities of slowly cooled (20 mK $\cdot$ min^{-1}) and rapidly cooled samples of κ-(BEDT-TTF)$_2$Cu[N(CN)$_2$]Br across T_g. They reported a similar analysis in the rapidly cooled sample and found that the analysis of electronic heat capacity strong coupling d-wave model holds for this rapidly cooled state, although the density of state reflected in γ-term is decreased down to 1/2. This fact implies that the pairing state does not change by the cooling rate.

In this section, we summarize the results of magnetic angle-resolved heat capacity measurements of κ-(BEDT-TTF)$_2X$ compounds. Using the relaxation technique, Malone *et al.* studied the in-plane magnetic field dependence of heat capacity at extremely low-temperature region below 1 K for κ-(BEDT-TTF)$_2$Cu[N(CN)$_2$]Br and κ-(BEDT-TTF)$_2$Cu(NCS)$_2$.[93] They observed clear fourfold symmetric oscillations in γ with the background twofold oscillations coming from the crystal. The fourfold oscillations arise from the existence of nodes in the superconductive states. Their results are suggestive of the d_{xy}-type node parameter of the superconductivity in these materials. Izawa *et al.* reported the fourfold oscillations predicting $d_{x^2-y^2}$ node parameter.[94] There is discrepancy between the peak angles of the fourfold oscillations in literature and Kuroki *et al.* predicted that the node direction can change depending on the magnitude of on-dimer Coulomb interaction determined by the transfer between two molecules forming the dimer unit in the κ-type compound.[95] More recently, the sign change in the fourfold oscillations depending on the temperature and magnetic fields of the experiments has been explained by Vorontsov and Vekhter.[96]

Since the pairing state is most plausibly the unconventional d-wave superconductivity, the k-type compound with 10 K transition also shows novel property at extremely high magnetic field region. Lortz *et al.*[97] measured the heat capacity of κ-(BEDT-TTF)$_2$Cu(NCS)$_2$ with applying magnetic field just parallel to the conducting layer. The 2D layered superconductors like the organic system have a cylindrical Fermi surface and possess a very large $H_{\rm orb}$. When the in-plane external fields exceed the Pauli limit value of $H_P = 21$ T, the superconductive state changes to an unusual one where part of the Cooper pairs are sacrificed to be normal. In this special situation, spatial modulation in the superconductive order parameter occurs in the real space and this state is called as the Fulde–Ferrell–Larkin–Ovchinnikov (FFLO) state. They performed heat capacity measurements with strong magnetic fields up to 28 T applied parallel to the plane and found that heat capacity peak changes from a second-order structure to drastic first-order structure peak around 23 T and H_{c2} becomes larger at low-temperature regions as predicted by FFLO theories. Bergk *et al.* reported more detailed information by combining magneto-torque measurement and heat capacity under magnetic fields up to 32 T and determined precise H–T phase diagram. In the high-field region, temperature dependence of H_{c2} line shows a large upturn as is expected for FFLO state.[98,99] Although the peak is so sharp and looks like first-order transition, the experiment by Lortz *et al.* is based on the analysis of the temperature dependence

of the heat capacity at several magnetic fields. The magnetic field sweeping of the AC heat capacity measurements with fixed temperature performed by Agosta *et al.*, detected the smaller anomaly but has clear hysteretic feature when getting across the boundary of the FFLO state.[100,101] In several organic superconductors such as λ-$(BETS)_2GaCl_4$, λ-$(BETS)_2FeCl_4$ and $(TMTSF)_2ClO_4$, the possibility of FFLO is discussed by other methods. The detailed thermodynamic measurements using single crystal is still under way.

To see the variation of the bulk feature of the transition and the variation of the superconductive characters in the phase diagram of κ-type complexes, the heat capacity measurements under controlled pressure are performed by Tokoro *et al.* in κ-$(BEDT\text{-}TTF)_2Ag(CN)_2H_2O$, κ-$(BEDT\text{-}TTF)_2Cu(NCS)_2$ and κ-$(BEDT\text{-}TTF_{1-x}BEDSe\text{-}TTF_x)_2Cu[N(CN)_2]Br$ systems with alternative temperature oscillation (AC) technique.[102,103] The substitution of BEDT-TTF by BEDSe-TTF molecules with less than 20% produces chemical pressure effects and decreases the transition temperature. Tokoro *et al.* studied the AC heat capacity under pressure and pursued the shift of thermal anomaly associated with superconductive transition. However, the background value is so large and it is still in the process to attain better resolution, since the lattice heat capacity above 5 K is very large in the organic systems. A new technique using microchip calorimeter was also performed for tiny sample of κ-$(BEDT\text{-}TTF)_2Cu[N(CN)_2]Br$ under magnetic fields using tiny crystals of few mg by Muraoka *et al.*[104] Although the 10 K-class superconductors show the strong coupling feature with large pair condensation energy, the pressure experiments indicate a kind of crossover from the strong coupling feature to the weaker one concomitant with the decrease of T_c. The consistency between the feature produced by applying the external pressures and that observed in the chemical pressure effect by the systematic change of the counter anions is being discussed in literatures.[105]

4. Thermodynamic Properties of π–d Systems Consisting of BETS and Counter Anions

The electronic structures of organic charge transfer complexes are determined by delicate balance of band energy W and on/intersite Coulomb energy expressed by U, V and electron–phonon interactions of π-electrons existing in low-dimensional crystal lattice. It is also emphasized that in these organic compounds, a rich variety of electronic and magnetic phases appear with the tuning of external parameters such as temperature (T), pressure (p), magnetic field (H), etc. This tendency appears drastically in π–d hybrid systems, where π-electrons in organic layers interact with magnetic spins of the counter anions possessing $3d$-electrons.

Studying the interplay of conductivity/superconductivity and magnetic features is an important subject for organic conducting systems. The competition and coexistence of superconductivity and magnetic ordering has been a long discussed problem in condensed matter physics. Furthermore, the tuning of physical properties by

changing magnetic fields in molecule-based functional materials gives challenging subjects for application as molecular devices. The magnetic interactions between π-electrons and d-electrons and possibility of π–d hybridization in electronic bands have been discussed for about 20 years mainly in charge transfer complexes of BETS and magnetic counter anions such as $FeBr_4^-$ and $FeCl_4^-$. These compounds possess κ-type and λ-type structures. In 2001, the appearance of magnetic field-induced superconductivity was reported by Uji *et al.* in λ-$(BETS)_2FeCl_4$ and its solid solution system with $GaCl_4^-$ anion.[106] In the case of λ-$(BETS)_2FeCl_4$, the antiferromagnetic transition of 3d-electrons occurs around 8.3 K. This transition appears simultaneously with the metal to insulator transition of π-electrons and the ground state is a kind of insulating state. However, by applying extremely large magnetic fields above 17 T which are applied just parallel to the 2D plane, the metallic conductivity recovers and field-induced superconductivity appears. This effect is explained by the Jaccarino–Peter compensation mechanism.[106] The 3d spins which ordered the antiferromagnetic structure change their orientation with the increase of external field. The insulating state of BETS layers produced by the strong π–d interactions changes to the conductive state at around 4–5 T. Under the application of extremely large magnetic field in the in-plane direction all 3d spins oriented in the same direction. The large internal magnetic field induced by the magnetic anions layer compensates the external field in the conducting π-electron layers. Above the critical field of 17 T, where this compensation effect works to cancel the magnetic field, the bulk superconductivity appears. The relatively strong coupling of the π–d interaction in this hybrid magnetic conductors makes the ground state quite complicated. On the other hand, coexistence of superconductivity and magnetic long-range ordering was found by Fujiwara and co-workers in Refs. 107–110 for κ-$(BETS)_2FeBr_4$ and κ-$(BETS)_2FeCl_4$. The magnetic field-induced superconductive phase is also reported in the κ-type BETS compound.

The thermodynamic measurements on κ-$(BETS)_2FeBr_4$ were performed in Ref. 106 for the first time. In this work, the single crystal of about 0.19 mg was measured down to 0.9 K by relaxation technique in a ^{3}He cryostat. Zero-field heat capacity shows a sharp anomaly at 2.4 K with λ-like structure, just as the same temperature where the step-like decrease of resistivity occurs with decreasing temperature. The temperature dependence of magnetic entropy obtained by integration of the C_pT^{-1} versus T curve with respect to temperature reaches to about 15 $J \cdot K^{-1} \cdot mol^{-1}$. This value corresponds to the full entropy of Fe^{3+} of Rln 6. The bulk ordering of 3d-electron spins was confirmed by this discussion. Application of magnetic fields of 0.1 T and 0.2 T perpendicular to the plane reduces the peak temperatures down to 2.36 K and 2.05 K, respectively, but the peak shape is retained as a sharp one typically realized in antiferromagnetic transitions. Otsuka *et al.* performed heat capacity measurement by adiabatic technique using 5.80 mg polycrystalline sample of κ-$(BETS)_2FeCl_4$ and obtained similar sharp heat capacity peak at 0.45 K, which is also consistent with the resistivity measurement.[109] This is also confirmed by Fukuoka *et al.*[111–113] In this case, the entropy value around the

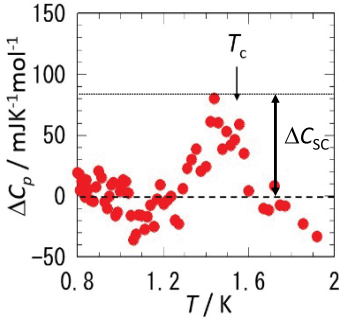

Fig. 10. (Color online) The temperature dependence of ΔC_p around the superconductive transition determined by subtracting the normal state data obtained under magnetic fields above H_{c2} from the 0 T data for the magnetic superconductor κ-$(BETS)_2FeBr_4$. Although there is a large background due to the antiferromagnetic component in the heat capacity, the subtraction of that gives similar order of heat capacity jump as compared with κ-$(BEDT\text{-}TTF)_2X$ superconductors with similar transition temperature.[112]

transition reaches to 81% at 1.5 T_N, suggesting a slight amount of low-dimensional character. The discussion including heat capacity and other experiments has been performed in Refs. 108 and 110. Although there are some attempts to detect thermal anomalies around the superconductive transition temperatures and quasi-particle excitations at low temperatures, the heat capacity of π-electrons is masked by huge magnetic contribution. The high-resolution heat capacity experiment by Fukuoka *et al.* succeeded to detect the superconductive transition and they claim that ΔC_p corresponding to the gap is of similar order with those of other BEDT-TTF complexes as shown in Fig. 10.[112] Fukuoka *et al.* also studied anisotropic behaviors against in-plane magnetic fields direction by heat capacity and anisotropic variations of Néel temperature and the superconductivity according to the difference of magnetic field directions.[111,113] The anisotropic feature versus the direction of the applied fields is shown in Fig. 11 for the case of κ-$(BETS)_2FeBr_4$. It is emphasized that no latent heat appears around the superconductive transition which is one of the evidences that the magnetic order and the superconductivity order coexist as a ground state. These complexes are considered as magnetic superconductors like in Chevrel compounds ($REMo_6S_8$) and $RERh_4B_4$ system, where RE denotes rare earth elements. The thermodynamic study around the superconductive transition and interplay of magnetism and superconductivity is a subject to be discussed in the near future by heat capacity measurements. The heat capacity of λ-type complexes of $(BETS)_2FeCl_4$ recently revealed curious thermodynamic behaviors which are peculiar for the organic π–d interacting system. This compound shows metal–insulator transition around 8 K. According to the magnetic properties measurements by Tokumoto *et al.*, AF ordering in Fe^{3+} takes place simultaneously with this transition.[114] The paramagnetic metal state above this temperature shows curious dielectric properties by microwave conductivity measurements.[115] The dimer-Mott physics in the π-electrons in conducting plane is considered as affecting the

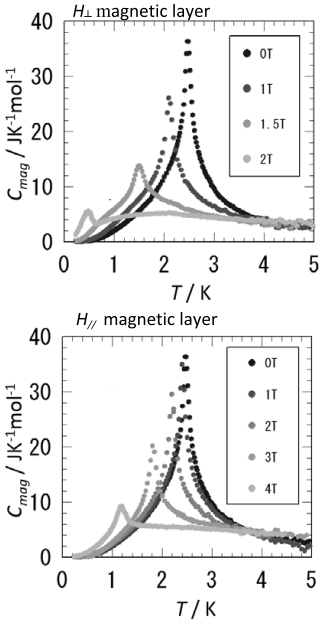

Fig. 11. The plots of temperature versus magnetic field dependence around the antiferromagnetic transition of κ-$(BETS)_2FeBr_4$. The magnetic fields are applied parallel to the (upper) a-axis (in-plane direction) and (lower) c-axis (out-of-plane direction). The latter is the hard axis of the magnetic transition.[111,113]

spin ordering in Fe^{3+} of d-electrons. Heat capacity measurement was performed by Negishi *et al.*, for the first time, and they reported that λ-like anomaly occurs around the magnetic ordering temperature of 8.3 K.[116] They indicated an anomalous hump in heat capacity around 4–7 K. They also suggested lattice instability at around 70 K consistent with dielectric measurements provided earlier by them. In 2009, Akiba *et al.* examined the heat capacity of λ-$(BETS)_2FeCl_4$ precisely and indicated that the low-temperature hump can be fitted by the Schottky splitting model for free Fe^{3+} in the effective internal field of 4 T.[117] This field corresponds to the $H_{\pi-d}$ field determined by the ordered π-electrons in the BETS layers, which means that the effective fields on the $3d$-electron in the $FeCl_4^+$ layer had arisen just by the π–d interactions. They also suggested that the $3d$ spins in the $FeCl_4^+$ anions are not ordered and behave as paramagnetic.[118] They suggested that the broad shoulder in the temperature dependence of magnetization at around 4–5 K of λ-$(BETS)_2FeCl_4$ observed by Tokumoto *et al.* in Ref. 114 is also related to the paramagnetic degrees of freedom of Fe^{3+} spins. The observation of internal magnetic fields by Mössbauer spectroscopy by Waerenborgh *et al.* indicates that the internal field of 4 T is consistent with their data.[119] The results by Akiba *et al.* raise an interesting possibility in π–d interacting system and the picture of magnetic ordering needs to be reconsidered. The magnetic ordering appearing concomitant with the metal–insulator transition is mainly dominated by the π-electrons with relatively

strong magnetic interactions between dimer units and the $3d$ spins involved in the magnetic order through the π–d interaction working locally. The larger entropy of the $3d$ spins survives even below T_N that gives contribution to the magnetic heat capacity at low-temperature region. The situation is quite different from κ-type complexes where distinct long-range ordering in $3d$ spins occurs as a bulk form. Concerning on the fact that field-induced superconductivity occurs above 17 T, there are no heat capacity experiments at present. This is because of the difficulty to realize the exact parallel configuration of external fields against the 2D plane, although the torque measurements are performed by Uji *et al.*, to evidence the occurrence of superconductivity under high magnetic fields.[106]

The superconductive transition of λ-$(BETS)_2GaCl_4$ has been studied by Ishizaki *et al.* by the peak analysis of superconductive transition.[120] This is not a π–d system and has bulk superconductivity of π-electrons with a transition temperature of about 5 K. They estimated thermodynamic parameters from a fitting of the heat capacity data above T_c and obtained $\gamma = 14.4 \pm 3.4\ \mathrm{mJ \cdot K^{-2} \cdot mol^{-1}}$ and $\beta = 14.5 \pm 0.1\ \mathrm{mJ \cdot K^{-4} \cdot mol^{-1}}$. The Debye temperature was evaluated as $\Theta_D = 197 \pm 0.4$ K, which is nearly 10% smaller than those of κ-type superconductors. The $\Delta C_p/\gamma T_c$ value is evaluated as 1.37 ± 0.32. Imajo *et al.* performed measurements and reported that the γ-value is about $23\ \mathrm{mJ \cdot K^{-2} \cdot mol^{-1}}$ and it is comparable with weak coupling region similar to the κ-type compounds with middle class transition temperature.[121] The low-temperature analysis recently performed by Imajo *et al.* revealed the nodal features produced by electron correlations.

5. Organic Superconductors

Study of organic superconductivity theory is among the most fruitful and promising trends of condensed matter. At present, many models of organic superconductivity clarifying its mechanism are available. The essential point is the nature of pairing of carriers. Among numerous models of organic superconductivity, it is worth to mention the following ones: the electron–phonon interaction model, exciton model, Mott–Hubbard model, electron correlation model and model involving magnetic fluctuations. A version of the classification of mechanisms of pairing for organic superconductors is shown here according to Refs. 122 and 124.

5.1. *Pairing mechanisms for organic superconductors*

Though the customary properties of organic substances are different from those of inorganic ones, it is quite natural that the descriptions of the phenomenon of superconductivity in both cases have many common features. Let us consider the models most popular at the present time. In addition to the ordinary BCS mechanism based on the electron–phonon interaction, we turn also to the magnetic, exciton, plasmon and bipolaronic mechanisms of pairing. All these models involve the conception of pairing with the subsequent formation of a Bose condensate (at certain temperatures T_c) regardless of the reasons for the attraction.

In the framework of BCS theory, the critical temperature T_c in the case of weak electron–phonon interaction is described by the formula

$$T_c = 1.14\Theta \exp(-1/N_0 V), \tag{1}$$

where $\Theta = \hbar\Omega_D/k_{\mathrm{B}}$, $\hbar\Omega_D$ is the Debye energy, N_0 is the density of states at the Fermi level and V is the attractive pairing potential acting between electrons.

The maximum critical temperature evaluated by the BCS theory is as high as 40 K. Therefore, we are faced with the question of other mechanisms of pairing leading to its more realistic value. The interaction of electrons is repulsive, i.e., one needs to seek a "transfer system" in metals, which is distinct from the phonon system. The general scheme of the interaction of electrons via a transfer system Y can be schematically presented as

$$\begin{cases} e_1 + Y \to e_1^1 + Y^*, \\ e_2 + Y^* \to e_2^1 + Y, \end{cases} \tag{2}$$

where e_i corresponds to an electron with momentum p_i, Y is the ground state and Y^* is the excited state of the transfer system.

This reaction results in that the system returns to the initial state, and the electrons make the exchange by momenta.

Such interaction leads to the attraction, and the critical temperature is given by the formula

$$T_c \sim \Delta E \exp(-1/\lambda),$$

where ΔE is the difference of energies of the states Y and Y^* and λ depends on the interaction of electrons with the system Y.[123]

5.2. *Exciton mechanisms of pairing*

The electron–phonon interaction should not be the unique cause for the pairing of electrons, according to the general principles concerning the "transfer system" in superconductors. Some other interactions can be suitable or dominant. In principle, the mechanism of superconductivity can be switched on by the bound electrons which interact with conduction electrons. The first exciton-based model, in which the pairing is realized due to electron excitations, was proposed by Little[133] for organic superconductors and Ginzburg and Kirzhnitz[123] for layered systems. In the construction of this model, it was necessary to assume the existence of two groups of electrons: one of them is related to the conduction band, where the superconducting pairing occurs due to the exchange of excitons which are excitations in the second group of almost localized electrons. In view of the many-band character of the electron spectrum, layered structure and other peculiarities of the electron subsystem in high-temperature superconductors, such a distribution of electron states is quite possible. This underlies the development of a lot of exciton models. The searches for superconductivity in organic materials were stimulated to a significant degree

by the idea of Little about a possibility of high-temperature superconductivity due to the excitonic mechanism of the Cooper pairing of electrons in long conducting polymeric chains containing lateral molecular branches — polarizers. Since the mass M of such excitonic excitations is small, it would be expected to observe a high value of the temperature $T_c \sim M^{-1/2}$. But this model was not practically realized, since high-energy intramolecular excitonic excitations cannot ensure the binding of electrons in pairs.

At the present time, a number of quasi-one-dimensional organic superconductors with metallic conductance have been synthesized. They pass to the superconducting state at $T = 10$ K. Crystals of similar organic superconductors consist of, as a rule, planar molecules packed in zigzag-like stacks which form chains. The good overlapping of electron wavefunctions of neighboring molecules in a stack ensures the metallic conductance along a chain. The overlapping of electron wavefunctions of neighboring chains is small, which leads to the quasi-one-dimensional character of the electron spectrum and to a strong anisotropy of electronic properties of a crystal. Up to now, no experimental proofs of a manifestation of the excitonic mechanism is such systems are available.

As an example of a laminar system, we mention a quasi-two-dimensional structure of the "sandwich" type (dielectric–metal–dielectric). In such structures, the Cooper pairing of electrons in a metal film occurs due to the attraction caused by their interaction with excitons in the dielectric plates.

5.2.1. *Little's model*

In 1964, Little[133] advanced the assumption about a possibility of high-temperature superconductivity in organic materials, which became a stimulus to the search for superconducting organic materials.

In Little's model, a linear macromolecule with a particular structure (conducting polymer with attached strongly polarizable side groups at its center; Fig. 12) was considered. Such molecule must generally contain the same basic elements as in a conducting metal.

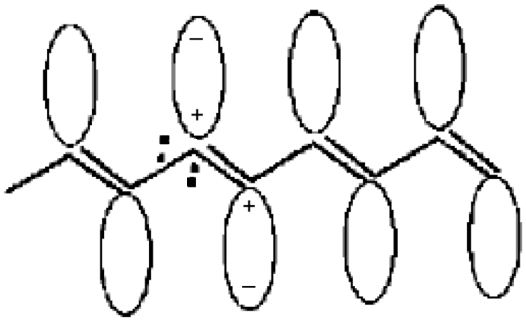

Fig. 12. Hypothetical superconducting molecule.

A medium, where the electrons would move freely as in a periodic lattice, and specific interactions of electrons with the molecule leading to the formation of electron pairs are needed. The molecule can consist of the basic chain of atoms connected by conjugate bonds, to which polarizable side radicals are attached.

It is known that the electrons move along a chain of conjugate double bonds freely like in a metal. The molecules in side chains (like diethylcyanonides) can be easily polarized, and the electrons in them can freely move from one side of molecules to another side.

When the electron bypasses each side chain, the field created by it polarizes the electron shell of side radicals and induces a positive charge at the end of the radical nearest to the chain. This polarization somewhat lags behind the motion velocity of the electron and is conserved at the passage of the second electron. The latter is attracted to the domains with a positive charge and indirectly to the first electron. In other words, the pairs can be formed during the motion of electrons along the molecule. The pairing occurs due to a displacement of electrons in side radicals.

We recall that, according to the BCS theory, the superconducting transition temperature is estimated by formula (1).

For Little's mechanism, the phonon frequency should be replaced by the significantly higher energies of electron excitations in side chains. Eventually, the physical reason consists in that the lighter electrons causing the polarization of side chains move significantly more rapidly than the atoms of the lattice in the case of the phonon mechanism. Respectively, the estimates of T_c for Little's mechanism give 300–2000 K. Thus, the superconductivity at high temperatures is possible in such systems, where the attractive electron–electron interaction is ensured by electron excitations, rather than by phonons.

Of course, this hypothetical model does not consider a number of factors able to change the main conclusion about a possibility of the superconductivity in organic polymers. These factors include, in the first turn, various instabilities such as, for example, the Peierls instability related to the impossibility for the metallic conduction and the superconductivity in a one-dimensional chain to exist. In addition, we note that the indicated model refers to an intramolecular process. However, in order to practically realize the superconductivity, it is necessary that the superconducting state be characteristic also of intermolecular processes. Thus, the main positions of Little's model are not indisputable. The value of Little's idea consists in the stimulation of theoretical and experimental works for systems with bounded dimensions, consideration of new mechanisms of superconductivity and search for new organic conductors.

As a result of these searches, a great number of organic conductors and superconductors were synthesized. We now list some superconductors: the superconducting polymer $(SN)_n$ with $T_c = 1$ K (quasi-one-dimensional superconductor) and quasi-two-dimensional organic superconductors of the type $(TMTSF)_2PF_6$ with T_c of about 12 K. Finally, the last achievement is related to the recent discovery of superconductivity in a three-dimensional lattice of fullerenes, which are purely

organic substances with a transition temperature of 18 K for K_3C_{60} and 45 K for $Rb_xTl_yC_{60}$. It is worth noting that T_c increases with the dimension. For low-dimensional superconductors, it is frequently necessary to apply a pressure in order to increase T_c. This can be understood by assuming that the pressure increases the overlapping of wavefunctions between chains or layers.

Separately, we consider the mechanism of superconductivity in fullerenes. It was shown that the temperature T_c in C_{60} doped in different ways correlates with the lattice parameter of an fcc lattice. In this case, T_c decreases with the distance between C_{60} atoms, which can be varied with the help of a change of the composition or the application of a high pressure. This dependence is determined by the overlapping between C_{60} atoms or by the density of states at the Fermi level N_0. In the BCS model, T_c depends on N_0 exponentially. The density of states decreases as the pressure increases (growth of the overlap between C_{60} atoms leading to an increase in the allowed energy bandwidth and to a decrease in N_0). In addition, the dependence of N_0 on the pressure was studied with the help of independent experiments (Knight shift). The obtained data give a possibility to estimate the phonon frequency $h\nu/k_B = 600$ K that is responsible for the pairing. This frequency is close to the frequency of high-frequency phonons inside C_{60}.

5.3. *Pairing symmetry*

In the description of organic superconductors, one of their crucial physical characteristics is the pairing symmetry or the symmetry of the order parameter. This question was considered at many conferences and workshops over the world. Several NATO workshops and conferences on this trend were held at Ukraine with the participation of and under the guidance of one of the authors of this work.[123–126]

The development of the microscopic theory of superconductivity was followed by the interest in the question about the nontrivial superconductivity corresponding to Cooper's pairing with nonzero orbital moment.

As is known, He^3 was the first system in which the nontrivial pairing was discovered. To explain this phenomenon, it was necessary to introduce a supplementing mechanism of pairing due to spin fluctuations.

5.4. *Order parameter of organic superconductors*

In the superconducting state, most physical properties depend on the symmetry of superconductor's order parameter, which is defined by the formula

$$\Delta_{\alpha\beta}(\mathbf{k}) = \langle a_{\alpha\mathbf{k}} a_{\beta-\alpha\mathbf{k}} \rangle \,. \tag{3}$$

The problem of pairing symmetry is the problem of the pairing of charged fermions into states with the final orbital moment.

As usual, both the standard pairing called the *s*-pairing and the nonstandard *d*-pairing are considered. They differ by the orbital moment of the pair: in the first and second cases, the moments are $L = 0$ and $L = 2$, respectively.

It should be recalled that the continuous symmetry group in crystals is broken, and we need to say not about the orbital moment, but about the irreducible representations, by which the order parameter is classified. We will consider this question in the following.

Frequently, the standard pairing, called the s-pairing, and the nonstandard pairing are distinguished. At the nonstandard pairing, the symmetry of the order parameter is lower than the symmetry of a crystal.

The possible symmetries of superconductor's order parameter for a two-dimensional tetragonal crystal (square lattice) were enumerated in monograph[122] on the basis of the theory of group Ackrepresentations. The basis functions of relevant irreducible representations define the possible dependence of the order parameter on the wave vector.

We emphasize that the anisotropic pairing with the orbital moment $L = 2$, i.e., $d_{x^2-y^2}$, has the following functional form in the k-space:

$$\Delta(\mathbf{k}) = \Delta_0[\cos(k_x a) - \cos(k_y a)], \tag{4}$$

where Δ_0 is the maximum value of the gap and a is the lattice constant. The gap is strongly anisotropic along the direction (110) in the k-space. In this case, the order parameter's sign is changed in the directions along k_x and k_y.

In addition to the d-symmetry, it is worth to consider the s-symmetry as well. In the last case, we can choose two collections of basis functions

$$\Delta(\mathbf{k}) = \Delta_0. \tag{5}$$

As for the anisotropic s-pairing, it was analyzed in the work by Anderson,[128] who has studied the mechanism of pairing on the basis of the tunneling of electrons between layers. In these states, the order parameter's sign is invariable, and its amplitude is varied along the direction (110):

$$\Delta_{\mathrm{an}\,s}(k) = \Delta_0[\cos(k_x a) - \cos(k_y a)]^4 + \Delta_1, \tag{6}$$

where Δ_1 corresponds to the minimum along the direction (110).

Based on the symmetry-based reasoning, we can conclude that the mixed states with various symmetries can be realized. We mention the states which are mostly in use. The "extended" s-coupled states were considered in work by Scalapino.[129] A possible functional form of these states is as follows:

$$\Delta_{\mathrm{ex}\,s}(k) = \Delta_0\{(1+\gamma^2)[\cos(k_x a) - \cos(k_y a)]^2 - \gamma^2\}. \tag{7}$$

They have eight parts with alternating signs and eight nodes which are split by $\pm\gamma\pi/2$ along the direction (110). Kotliar and co-workers used mixed $s+id$ states[129]:

$$\Delta_{s+id}(k) = \Delta_0[\varepsilon + i(1-\varepsilon)[\cos(k_x a) - \cos(k_y a)]]. \tag{8}$$

Laughlin[130] analyzed the mixed states $d_{x^2-y^2} + id_{xy}$ on the basis of the anyonic mechanism of pairing:

$$\Delta_{d+id}(k) = \Delta_0[(1-\varepsilon)[\cos(k_x a) - \cos(k_y a)] + i\varepsilon[2\sin(k_x a)\sin(k_y a)]], \tag{9}$$

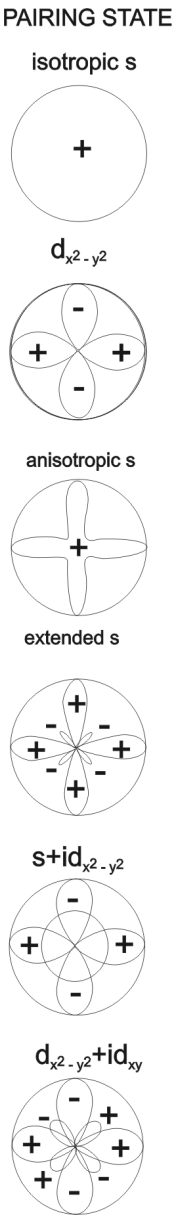

Fig. 13. Kinds of pairing symmetry which are considered for organic superconductors.

where ε is the share of s or d_{xy} states mixed with the $d_{x^2-y^2}$ states and $\varepsilon\Delta_0$ is the minimum value of the energy gap. These mixed states are of interest, because they are not invariant with respect to the inversion in the time. The value and phase of superconductor's order parameter as functions of the direction in cuprate planes CuO_2 are given in Fig. 13 for various kinds of the pairing symmetry.

5.5. *Symmetry-based classification of order parameters*

We recall again that there is no classification of states by the orbital moment for crystals. So, the point symmetry groups should be used while developing the general theory of nonstandard pairing. The classification of superconducting states by the irreducible representations of groups for high-temperature superconductors was constructed, in particular, by Annett who was one of the pioneer researchers in this field.[131] As for superconductors with heavy fermions, the group analysis was carried out in Ref. 132.

In this case, we should like to mention the question of whether the symmetry of the order parameter in organic is lower than the symmetry of the crystal lattice.

The order parameter can be represented as a linear combination

$$\Delta_k = \sum \eta_{\Gamma_i} f_{\Gamma_i}(k), \tag{10}$$

where η_{Γ_i} is the irreducible representation of groups, by which the order parameter is transformed, f_{Γ_i} denotes the basis functions of the irreducible representation, A_{1g} corresponds to the anisotropic s-symmetry and B_{1g} corresponds to the d-pairing. An analogous decomposition of the order parameter was performed in the case of superconductors with heavy fermions UPt_3. The symmetric states of the system can be presented by the indication of all possible subgroups of the full group, relative to which the order parameter is invariant.[94] The full symmetry group of a crystal includes a point symmetry group G, operations of inversion of the time R and the group of calibration transformations $U(1)$. Thus, we have the following partition into subgroups:

$$G \times R \times U(1). \tag{11}$$

The La- and Y-based superconductors, which have the tetragonal symmetry of crystal lattices, i.e., $G = D_{4h} = D_4 \times I$,[124] are mostly studied. In the Y-based compounds, one observes small orthorhombic distortions of a crystal lattice.

Group D_{4h} includes the operations of rotations C_n around the z-axis by the angles $\pi n/2$ and rotations U_n by the angle π:

$$x\cos(\pi n/2) + y\cos(\pi n/2), \tag{12}$$

where $n = 0, 1, 2, 3$ have five reducible representations: four one-dimensional representations (A_{1g}, A_{2g}, B_{1g} and B_{2g}) and one two-dimensional (E) representation.

In Ref. 134, it was shown that the superconducting gap in organic conductors like κ-(BEDT-TTF)$_2X$ has the symmetry of the orthorhombic point group D_{2h}.

Thus, we may note that the symmetry of organic superconductors is lower than the symmetry of high-temperature superconductors.

6. Conclusions

Systematic survey of materials and detailed thermodynamic properties peculiar for quasi-one-dimensional and quasi-two-dimensional organic conductors and superconductors mainly for dimer-Mott-type compounds are reported. The variety of crystal

structures in TMTSF-, TMTTF-, BEDT-TTF- and BETS-based charge transfer complexes with various types of counter anions give the characteristic appearance manners of electron correlations in molecular conductors. In the case of the quasi-one-dimensional TMTSF/TMTTF complexes, heat capacity measurements detect superconductive transition with bulk characters. However, the disorders in anions sensitively affect the thermodynamic properties through various mechanisms. The drastic lattice dynamics probably related to charge fluctuations is also the feature of these compounds. In the case of BEDT-TTF and BETS compounds, the phase relation of the superconductive phase is controlled by quantum mechanical feature related to onsite and intersite Coulomb parameters and bandwidth. The possibility of d-wave pairing is suggested based on the physics of effectively half-filled states peculiar for dimer-Mott-type compounds. The theoretical models for the organic systems are also introduced. The organic superconductivity is a dynamical field of solid-state physics which is intensively developed by theorists and experimentalists. They gather most of the relevant problems in modern condensed matter physics. This subject studied for over three decades still holds a very promising future providing new idea and new philosophy in electrons with relatively light masses. The quantum mechanical freedoms such as spins, charges and lattices and their combinations give unexpected features in superconductivity different from d- and f-electron systems. Presently, systematic research from both experimental and theoretical sides of organic superconductors is in progress. By summarizing the thermodynamic properties and the arguments on mechanisms of superconductivity in organic superconductors, we expect that further investigations for new aspects of organic superconductors would be accelerated. The developments of systematic thermodynamic measurements combined with other experimental and theoretical studies are necessary for this purpose.

Acknowledgments

This work was partly supported by CREST, JST Program in the area of "Establishment of Molecular Technology towards the Creation of New Functions." The work in the theoretical part was partially supported by the National Academy of Sciences of Ukraine (Project No. 0116U002067). The authors also thank the JSPS support through the JSPS Invitation Fellowship Program for Research in Japan under the Grant No. S-15766. One of the author S. Kruchinin acknowledges Research Center for Structural Thermodynamics, Graduate School of Science, Osaka University, for giving an opportunity to stay as a Guest Professor for collaboration.

References

1. H. Akamatsu, H. Inokuchi and Y. Matsunaga, *Nature* **173**, 168 (1954).
2. R. C. Haddon *et al.*, *Nature* **350**, 320 (1991).
3. T. T. M. Palstra *et al.*, *Solid State Commun.* **93**, 327 (1995).
4. M. S. Dresselhause and G. Dresselhause, *Adv. Phys.* **51**, 1 (2002).

5. T. Weller *et al.*, *Nat. Phys.* **1**, 39 (2005).
6. A. Fujiwara *et al.*, *Nature* **464**, 76 (2000).
7. T. Ishiguro, K. Yamaji and G. Saito, *Organic Superconductors* (Springer, Heidelberg, 1998).
8. J. M. Williams *et al.*, *Organic Superconductors* (Prentice-Hall, New Jersey, 1992).
9. P. Bernier, S. Lefrant and G. Bidan (eds.), *Advances in Synthetic Metals* (Elsevier, 1999).
10. H. Klank, *Organic Electronics: Materials, Manufacturing and Application* (Wiley-VCH Verlag, Weinheim, 2005).
11. Z. Bao and J. Locklin, *Organic Field-Effect Transistors*, Optical Science and Engineering Series (CRC Press, London, 2007).
12. E. S. R. Gopal, *Specific Heats at Low Temperature* (Heywood Books, London, 1966).
13. M. Sorai, *Comprehensive Handbook of Calorimetry and Thermal Analysis* (Wiley, New York, 2004).
14. H. Kino and H. Fukuyama, *J. Phys. Soc. Jpn.* **64**, 1877 (1995); *ibid.* **65**, 2158 (1996).
15. H. Seo, C. Hotta and H. Fukuyama, *Chem. Rev.* **104**, 5005 (2004).
16. H. Mori, *J. Phys. Soc. Jpn.* **75**, 051003 (2006).
17. D. Jérome, *Science* **252**, 1509 (1991).
18. V. A. Bondarenko *et al.*, *Synth. Met.* **120**, 1039 (2001).
19. S. Uji *et al.*, *Phys. Rev. Lett.* **105**, 267201 (2010).
20. N. Thorup *et al.*, *Acta. Crystallogr. B* **37**, 1236 (1981).
21. D. Jérome *et al.*, *J. Phys. Lett. (Paris)* **41**, L95 (1980).
22. K. Bechgaard *et al.*, *Phys. Rev. Lett.* **46**, 852 (1981).
23. L. Degiorgi and D. Jérome, *J. Phys. Soc. Jpn.* **75**, 051004 (2006).
24. P. Garoche, R. Brusetti and K. Bechgaard, *Phys. Rev. Lett.* **49**, 1346 (1982).
25. P. Garoche *et al.*, *J. Phys. Lett. (Paris)* **43**, L147 (1982).
26. R. Brusetti, P. Garoche and K. Bechgaard, *J. Phys. C, Solid State Phys.* **16**, 3535 (1983).
27. S. Yonezawa, Y. Maeno and D. Jérome, *J. Phys., Conf. Ser.* **449**, 012032 (2013).
28. P. Garoche and F. Pesty, *J. Magn. Magn. Mater.* **54–57**, 1418 (1986).
29. F. Pesty, G. Faini and P. Garoche, *J. Appl. Phys.* **63**, 3061 (1988).
30. T. Konoike, K. Uchida and T. Osada, *Physica B* **405**, S104 (2010).
31. N. A. Fortune *et al.*, *Phys. Rev. Lett.* **64**, 2054 (1990).
32. H. Yang, J. C. Lasjaunias and P. Monceau, *J. Phys., Condens. Matter* **12**, 7183 (2000).
33. F. Pesty, P. Garoche and A. Moradpour, *Mol. Cryst. Liq. Cryst.* **119**, 251 (1985).
34. S. Morishita *et al.*, *J. Therm. Anal. Calorim.* **123**, 1877 (2016).
35. M. Chung *et al.*, *Phys. Rev. B* **48**, 9256 (1993).
36. J. Coroneus, B. Alavi and S. E. Brown, *Phys. Rev. Lett.* **70**, 2332 (1993).
37. J. Odin *et al.*, *Solid State Commun.* **91**, 523 (1994).
38. D. K. Powell *et al.*, *Solid State Commun.* **119**, 637 (2001).
39. J. C. Lasjaunias *et al.*, *Solid State Commun.* **84**, 297 (1992).
40. K. Biljaković, J. C. Lasjaunias and P. Monceau, *Synth. Met.* **71**, 1849 (1995).
41. J. C. Lasjaunias *et al.*, *Phys. Rev. Lett.* **72**, 1283 (1994).
42. J. C. Lasjaunias *et al.*, *Eur. Phys. J. B* **7**, 541 (1999).
43. J. C. Lasjaunias *et al.*, *Synth. Met.* **103**, 2130 (1999).
44. J. C. Lasjaunias, K. Biljaković and P. Monceau, *Phys. Rev. B* **53**, 7699 (1996).
45. J. C. Lasjaunias *et al.*, *J. Low Temp. Phys.* **130**, 25 (2003).
46. J. C. Lasjaunias *et al.*, *J. Phys. IV (France)* **12**, 23 (2002).
47. H. Yang, J. C. Lasjaunias and P. Monceau, *J. Phys., Condens. Matter* **11**, 5083 (1999).

48. J. C. Lasjaunias *et al.*, *J. Phys., Condens. Matter* **14**, 837 (2002).
49. V. A. Bondarenko *et al.*, *Synth. Met.* **103**, 2218 (1999).
50. T. Yamaguchi *et al.*, *Synth. Met.* **103**, 2210 (1999).
51. R. Mélin *et al.*, *Phys. Rev. Lett.* **97**, 227203 (2006).
52. S. Sahling *et al.*, *Eur. Phys. J. B* **59**, 9 (2007).
53. K. Biljaković *et al.*, *Synth. Met.* **159**, 2402 (2009).
54. M. de Souza *et al.*, *Physica B* **404**, 494 (2009).
55. K. Kanoda, *Hyperfine Interact.* **104**, 235 (1997).
56. K. Kanoda, *Physica C* **287**, 299 (1997).
57. K. Miyagawa, K. Kanoda and A. Kawamoto, *Chem. Rev.* **104**, 5635 (2004).
58. K. Kanoda, *J. Phys. Soc. Jpn.* **75**, 051007 (2006).
59. B. Andraka *et al.*, *Phys. Rev. B* **40**, 11345 (1989).
60. B. Andraka *et al.*, *Solid State Commun.* **79**, 57 (1991).
61. Y. Nakazawa and K. Kanoda, *Phys. Rev. B* **53**, R8875 (1995).
62. Y. Nakazawa and K. Kanoda, *Synth. Met.* **103**, 1903 (1999).
63. H. Taniguchi *et al.*, *J. Phys. Soc. Jpn.* **74**, 468 (2003).
64. H. Taniguchi, A. Kawamoto and K. Kanoda, *Phys. Rev. B* **67**, 014510 (2003).
65. H. Akutsu, K. Saito and M. Sorai, *Phys. Rev. B* **61**, 1414 (2000).
66. H. Akutsu *et al.*, *J. Phys. Soc. Jpn.* **68**, 1968 (1999).
67. Y. Nakazawa and K. Kanoda, *Phys. Rev. B* **60**, 4263 (1999).
68. Y. Nakazawa *et al.*, *Phys. Rev. B* **61**, R16295(R) (2000).
69. Y. Nakazawa *et al.*, *Physica B* **281–282**, 899 (2000).
70. O. J. Taylor, A. Carrington and J. A. Schlueter, *Phys. Rev. B* **77**, 060503 (2008).
71. H. Oike *et al.*, *Nat. Commun.* **8**, 756 (2017).
72. R. N. Lyubovskaya *et al.*, *JETP Lett.* **46**, 188 (1987).
73. A. Naito *et al.*, *Phys. Rev. B* **71**, 054514 (2005).
74. A. Naito *et al.*, *Synth. Met.* **388**, 595 (2003).
75. S. Yamashita *et al.*, *J. Therm. Anal. Calorim.* **81**, 591 (2005).
76. S. Katsumoto *et al.*, *J. Phys. Soc. Jpn.* **57**, 3672 (1988).
77. J. E. Graebner *et al.*, *Phys. Rev. B* **41**, 4808 (1990).
78. J. Wosnitza *et al.*, *Phys. Rev. B* **50**, 12747 (1994).
79. J. Wosnitza *et al.*, *Synth. Met.* **70**, 829 (1995).
80. T. Ishikawa *et al.*, *J. Therm. Anal. Calorim.* **92**, 435 (2008).
81. S. Imajo *et al.*, *Int. J. Mod. Phys. B* **30**, 1642014 (2016).
82. J. Wosnitza *et al.*, *Solid State Commun.* **98**, 21 (1996).
83. Y. Nakazawa and K. Kanoda, *Phys. Rev. B* **55**, R8670 (1997).
84. Y. Nakazawa and K. Kanoda, *Physica C* **282–287**, 1897 (1997).
85. T. Arai *et al.*, *Phys. Rev. B* **63**, 104518 (2001).
86. K. Kanoda *et al.*, *Phys. Rev. B* **54**, 76 (1996).
87. H. Mayaffre *et al.*, *Europhys. Lett.* **28**, 205 (1994).
88. S. M. De Soto *et al.*, *Phys. Rev. B* **52**, 10364 (1995).
89. H. Elsinger *et al.*, *Phys. Rev. Lett.* **84**, 6098 (2000).
90. J. Müller *et al.*, *Phys. Rev. B* **65**, 140509 (2002).
91. S. Yamashita *et al.*, *Thermochim. Acta* **431**, 123 (2005).
92. O. J. Taylor, A. Carrington and J. A. Schlueter, *Phys. Rev. Lett.* **99**, 057001 (2007).
93. L. Malone *et al.*, *Phys. Rev. B* **82**, 014522 (2010).
94. K. Izawa *et al.*, *Phys. Rev. Lett.* **88**, 27002 (2002).
95. K. Kuroki *et al.*, *Phys. Rev. B* **B65**, 100516 (2002).
96. A. B. Vorontsov and I. Vekhter, *Phys. Rev. B* **75**, 224502 (2007).
97. R. Lortz *et al.*, *Phys. Rev. Lett.* **99**, 17002 (2007).

98. B. Bergk *et al.*, *Physica C* **470**, S586 (2010).
99. B. Bergk *et al.*, *Phys. Rev. B* **83**, 064506 (2011).
100. C. C. Agosta *et al.*, *Phys. Rev. B* **85**, 214514 (2012).
101. C. C. Agosta *et al.*, *Phys. Rev. Lett.* **118**, 267001 (2017).
102. N. Tokoro *et al.*, *J. Phys., Conf. Ser.* **132**, 012010 (2008).
103. N. Tokoro *et al.*, *Physica B* **405**, S273 (2010).
104. Y. Muraoka *et al.*, *Thermochim. Acta* **532**, 88 (2012).
105. Y. Muraoka *et al.*, *J. Therm. Anal. Calorim.* **123**, 1891 (2016).
106. S. Uji *et al.*, *Nature* **410**, 908 (2001).
107. H. Fujiwara *et al.*, *J. Am. Chem. Soc.* **123**, 306 (2001).
108. H. Fujiwara and H. Kobayashi, *Bull. Chem. Soc. Jpn.* **78**, 1181 (2005).
109. T. Otsuka *et al.*, *J. Solid State Chem.* **159**, 407 (2001).
110. H. Kobayashi *et al.*, *Synth. Met.* **133–134**, 477 (2003).
111. S. Fukuoka *et al.*, *Phys. Status Solidi C* **9**, 1174 (2012).
112. S. Fukuoka *et al.*, *J. Phys. Soc. Jpn.* **86**, 014706 (2017).
113. S. Fukuoka *et al.*, *Phys. Rev. B* **93**, 2451362016 (2016).
114. M. Tokumoto *et al.*, *Synth. Met.* **86**, 2161 (1997).
115. H. Matsui *et al.*, *Synth. Met.* **133–134**, 559 (2003).
116. E. Negishi *et al.*, *Synth. Met.* **133–134**, 555 (2003).
117. H. Akiba *et al.*, *J. Phys. Soc. Jpn.* **78**, 033601 (2009).
118. H. Akiba *et al.*, *J. Phys. Soc. Jpn.* **80**, 063601 (2011).
119. J. C. Waerenborgh *et al.*, *Phys. Rev. B* **81**, 060413(R) (2010).
120. Y. Ishizaki *et al.*, *Synth. Met.* **133–134**, 219 (2003).
121. S. Imajo *et al.*, *J. Phys. Soc. Jpn.* **85**, 043705 (2016).
122. S. Kruchinin, H. Nagao and S. Aono, *Modern Aspects of Superconductivity: Theory of Superconductivity* (World Scientific, Singapore, 2010).
123. V. L. Ginzburg and D. A. Kirzhnitz (eds.), *High-Temperature Superconductivity* (Consultants Bureau, New York, 1982).
124. A. A. Abrikosov, *Fundamentals of the Theory of Metals* (North-Holland, Amsterdam, 1998).
125. S. P. Kruchinin, *Rev. Theor. Sci.* **2**, 124–145 (2014).
126. M. Ausloos and S. Kruchinin (eds.), *Symmetry and Pairing in Superconductors* (Kluwer Academic Publishers, Dordrecht, 1999).
127. J. Annett and S. Kruchinin (eds.), *New Trends in Superconductivity*, (Kluwer Academic Publishers, Dordrecht, 2002).
128. S. Kruchinin, *Mod. Phys. Lett. B* **17**, 393 (2003).
129. M. Sigrist and T. M. Rice, *Rev. Mod. Phys.* **67**, 503 (1995).
130. P. W. Anderson, *Science* **4**, 1196 (1987).
131. S. Kruchinin and H. Nagao, *Int. J. Mod. Phys. B* **26**, 1230013 (2012).
132. J. Schmalian, *Phys. Rev. Lett.* **81**, 4232 (1998).
133. W. A. Little, *Phys. Rev. A* **134**, 1416 (1964).
134. M. Dion *et al.*, *Phys. Rev. B* **80**, 220511 (2009).